THE SPECTRAL MODELING TOOLBOX: A SOUND ANALYSIS/SYNTHESIS SYSTEM

A Thesis

Submitted to the Faculty

in partial fulfillment of the requirements for the

degree of

Master of Arts

in

ELECTRO-ACOUSTIC MUSIC

by

Micah Kimo Johnson

DARTMOUTH COLLEGE

Hanover, New Hampshire

May 29, 2002

Examining Committee:

(Chair) Larry Polansky

Eric Lyon

Metin Akay

Carol Folt
Dean of Graduate Studies

© 2002 Micah Kimo Johnson
All Rights Reserved

Abstract

This thesis describes the Spectral Modeling Toolbox, a collection of functions for digitally analyzing and synthesizing sound. The techniques in the Toolbox generalize the concepts of other analysis/synthesis systems in an environment created for algorithm design and research. The design decisions and basic techniques are documented in this thesis, and complete source code for the Toolbox is available. The Spectral Modeling Toolbox is an introduction to analysis/synthesis techniques, a spectral processing tool, and perhaps, the foundation for future sound recognition systems.

Acknowledgments

I would like to thank Larry Polanksy, Jon Appleton, Eric Lyon, and Charles Dodge for changing the way I think about music and for providing the supportive environment in which I produced this work.

I would also like to thank Metin Akay for pushing my research along and for believing that I could solve problems even when I could not see the solution.

Finally, I would like to thank my parents for encouraging me and never trying to limit my aspirations.

This thesis is dedicated to Amity, whose love and patience inspire me.

Contents

List of Tables

List of Figures

1 Introduction

Sound begins with a vibration. The vibration pushes and pulls on the surrounding air molecules, creating small variations in air pressure that travel away from the vibration as a sound wave. If we are in the path of the sound wave, the pressure variations move down our ear canal to our eardrum. The auditory system converts the vibration of the eardrum into nerve firings, which our brain arranges into auditory sensations. By deciphering the air pressure patterns we learn that a car passed by outside or that a neighbor is mowing his lawn.

Most people do not consider the complexity of sound perception because of the ease with which it occurs. We are surrounded by sounds all day long and it usually requires little effort to separate them into objects or events [1, p. 180]. Sound recognition also occurs with ease; we rarely confuse a cat's meow for a dog's bark. The ability to separate and recognize sound sources is important to our perception of music. It allows us to separate the sound of a soloist from the sound of the accompaniment and to distinguish a string quartet from a brass quartet.

How did we learn to separate and recognize sounds? Gestalt psychologists believe that we are born with an understanding of the basic laws of perceptual organization [2, p. 39–40]. These laws influence the learning process by enabling us to parse our auditory environment. From birth, we learn to organize sounds and the ease with which perception occurs later in life is the result of years of work.

The auditory system can also be trained to recognize small details in a sound. For example, some musicians can distinguish between the sound of a coronet and the sound of a trumpet. Music students who have taken several semesters of ear training can identify many different chords and intervals; some can even

transcribe four-voice chorals. In the last example, there is a conscious effort to train the auditory system to recognize sounds. It is a difficult task for many, but it is possible with enough practice.

While training our auditory system to recognize sounds may be difficult, training a computer to recognize sounds is even more complex. This is true for many tasks that fall under the category of artificial intelligence; it is difficult to program current computers to imitate human thought. Of course, computers can perform tasks that are nearly impossible for humans: try finding the next prime number after $2^{13,466,917} - 1$. Someday, I believe computer systems will be able to recognize and separate sound sources. One approach towards this goal is to use knowledge of the auditory system in the design of these systems.

1.1 Representations of Sound for Artificial Recognition

This thesis describes a sound analysis and synthesis system that incorporates knowledge of the auditory system. Analysis/synthesis systems are powerful sound processing tools: they can decompose sounds into simple components and synthesize sounds from these components.

Analysis/synthesis systems are often used for psychoacoustic research and music composition. They have been used in studies on instrument timbre to reduce sounds to basic elements and then to synthesize sounds from these elements. A human can then compare the synthesized sound to the original to determine if the basic elements completely describe the sound. In music composition, they allow for various sound processing and transformation techniques. Time scaling, pitch shifting, cross synthesis, and spectral morphing are all possible with these systems. Analysis/synthesis systems could also be the first step towards artificial recognition of sound sources since most of the information extracted by such systems is important to perception.

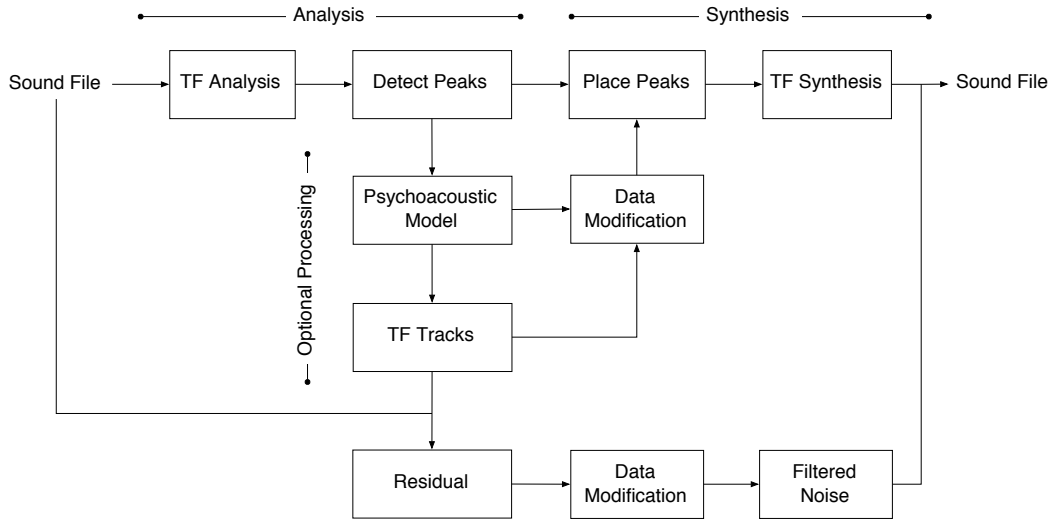

Figure 1.1: The Spectral Modeling Toolbox.

1.2 An Overview of the Spectral Modeling Toolbox

The sound analysis/synthesis system described in this thesis builds upon ideas from the McAulay-Quatieri analysis/synthesis system (MQ) and Xavier Serra's Spectral Modeling Synthesis (SMS). Figure 1.1 gives an overview of the system, called the Spectral Modeling Toolbox. A sampled sound is first transformed into a two-dimensional time-frequency representation. Next, regions of high time-frequency energy, called peaks, are detected and stored. A psychoacoustic model can be used to remove peaks that our auditory system cannot detect and time-frequency tracks can be formed from the remaining peaks. The synthesis stage creates peaks in a spectral buffer and takes the inverse time-frequency transform to create a new sound file.

While the Spectral Modeling Toolbox is a complete analysis/synthesis system, it is actually designed to be a development environment for these systems. The Toolbox generalizes the concepts of MQ and SMS and any stage of the process can be modified or reimplemented. The main goal is a flexible and open framework that is a suitable environment for algorithm design and research.

The Toolbox is distributed as a collection of MATLAB functions complete with source code and documentation.

I chose to implement the Toolbox in MATLAB because of the high degree of functionality already available in it. MATLAB is a commercial product designed for mathematical computation, analysis, visualization, and algorithm development. It has many functions that handle everything from simple plotting to statistical analysis and signal processing. There are also toolboxes available that extend its features to include wavelets, neural networks, curve fitting, and other specialized tasks.

The major disadvantage of the MATLAB platform is efficiency; the same algorithms written in C++ would be much faster. Since the Toolbox is meant to be an environment for research, efficiency is sacrificed to gain functionality. The tools available in MATLAB facilitate algorithm development and once these algorithms function properly, they can be coded in another language to improve efficiency.

While the primary goal was to create a flexible analysis/synthesis environment, this thesis can also serve as a reference for designers of sound processing systems. All of the details—from design decisions, to mathematical proofs and source code—are included. For those interested in exploring sound analysis in detail, the appendices are written as a tutorial to basic analysis techniques in MATLAB.

1.3 Thesis Structure

The remainder of the thesis is organized as follows:

- Chapter 2 introduces the mathematics behind time-frequency analysis of sound. Two techniques for representing sound in time and frequency are discussed in detail and compared.

- Chapter 3 presents extensions to the time-frequency techniques of Chapter 2. Three systems that influenced the design of the Spectral Modeling Toolbox are discussed and a global view of the Toolbox is given.

- Chapter 4 describes how to use the different functions available in the Toolbox. The current data structures are described in detail so that additional functions can be easily added to the Toolbox.

- Chapter 5 summarizes the work and discusses future directions for this project and analysis-synthesis systems in general.

- Appendix A is a tutorial that covers basic signal processing in MATLAB. Representations of sampled sound and the Fast Fourier Transform (FFT) are discussed.

- Appendix B documents techniques for extracting accurate frequency, amplitude, and phase information from the FFT.

- Appendix C is a catalog of relevant mathematical proofs and equations.

2 Signals in Time and Frequency

If we use the auditory system as a guide for designing sound analysis techniques, one point is clear: the importance of representing frequency. From the inner ear up to the brain—where our auditory system performs the sound analysis—frequency information is maintained [1, p. 532]. At the same time, the auditory system is sensitive to time information: we can hear separations between sounds as small as 50 ms [1, p. 385]. These two requirements suggest that time-frequency representations are appropriate tools for sound analysis.

The importance of frequency information to perception has been known for over one hundred years. In the nineteenth century, Helmholtz proposed that an instrument's timbre was related to the relative amplitudes of its harmonics. This is essentially true and it was not until the 1960s that researchers, attempting to synthesize instrument timbre on a computer, realized the importance of time-varying harmonics. Since then, time-frequency analysis techniques have been essential tools in audio signal processing.

Time-frequency analysis is simply a mathematical process that converts a time-domain signal (such as a sound) into a two-dimensional representation with time along one dimension and frequency along the other. This conversion relies on a set of functions, called *basis* functions, that can be combined to describe a signal. The Short-Time Fourier Transform (STFT) and the Continuous Wavelet Transform (CWT) are two examples of time-frequency transforms and they rely on different basis functions to create their representations. For the STFT, the basis functions are windowed sinusoids and for the CWT, the basis functions are dilated and translated versions of a "wavelet prototype." Because they use different basis functions, these two techniques offer different views of the information in the signal.

Before discussing the two transforms in detail, I will briefly review the concept of a basis because it is essential to understanding the similarities and differences between these two transforms.

2.1 A Basis for a Space

A basis for a space is a collection of elements that can be combined to describe any point in the space. We can think of a basis as a list of basic ingredients for making something.

Suppose we want to make a cake. A basis for the set of all cakes would include the following ingredients: flour, eggs, sugar, salt, baking powder, and butter. It would also include many more ingredients because we are considering the set of *all* cakes and some people put strange things in cakes. The basis, our list of all possible ingredients, must be complete so that it can describe any cake in the set of all cakes.

Once we have the list of all possible ingredients, a particular cake can be represented by a set of amounts for each of the ingredients. For example, a carrot cake has 1.5 cups of sugar, 3 eggs, 2 cups of flour, 5 carrots, etc.; while a pound cake has 2.5 cups of sugar, 5 eggs, 3 cups of flour, 0 carrots, etc. By thinking of cakes as lists of amounts, we can compare cakes by looking at the differences in the amounts of the ingredients. With these two cakes, the pound cake has more sugar, eggs, and flour, while the carrot cake has, obviously, more carrots. We can measure the *distance* between two cakes by finding the total of the differences between the ingredients. I will call the set of all cakes together with a distance function, a *space* of cakes.[1] If we think of the space of cakes, then a particular cake is a *point* in the space.

[1]The set of cakes with an appropriate distance function d could be a *metric* space if the distance function returns a nonnegative number for any two cakes in the space. It must also satisfy the following conditions for any three cakes x, y, and z: 1) $d(x, y) = 0$ if and only if $x = y$; 2) $d(x, y) = d(y, x)$; and 3) $d(x, y) + d(y, z) \geq d(x, z)$.

Something that has not yet been invented for cakes is a machine that can take a cake and determine the amounts of each ingredient. This machine could help us figure out a neighbor's secret recipe or determine why one restaurant's black forest cake tastes better than another's. While such a device does not exist in the world of baking, there are many such devices, called transforms, in the world of mathematics.

Instead of imagining the space of all cakes, imagine the space of all functions. Though less appetizing, the space of all functions has an interesting property not available in the space of cakes: there is more than one basis for the space. This means that completely different elements can be used to build the same function. For cakes, I guess you could make a devil's food cake from flour, chocolate, eggs, etc.; or a box mix, oil, and water. Therefore, the box mix, oil, and water could be another basis for the space of cakes. This analogy does not work, however, since the cake made from the box mix will taste different from the "real" cake. In the space of functions, different bases can be used to create exactly the same function.

As mentioned above, there are mathematical transforms that can determine the amount of each basis element present in any function. The general form of such transforms is shown below in (2.1), where $f(t)$ is the function, $g(t)$ is an element of the basis, and the line denotes complex conjugation (in case the basis function is complex valued). The integral of a product of functions is called an *inner product*, so decomposing a function onto a basis is nothing more than taking the inner product of the function with each element of the basis. The form of (2.1) will be seen in the formulas for both the STFT and the CWT.

$$\int f(t)\overline{g(t)}dt \tag{2.1}$$

2.2 Short-Time Fourier Transform

Since the Short-Time Fourier Transform is a time-varying extension of the Fourier Transform, I will briefly discuss the Fourier Transform.

The Fourier Transform of a function $x(t)$ is shown in (2.2) [3, p. 83]. If we compare the forms of (2.2) and (2.1), we can see that the Fourier Transform is the inner product of the function $x(t)$ with the basis functions $e^{i\omega t}$ (the minus sign comes from complex conjugation). In other words, a basis for the space of functions is the set of complex sinusoids of the form $e^{i\omega t}$, where ω is frequency.

$$X(\omega) = \int x(t)e^{-i\omega t}dt \tag{2.2}$$

The integral in (2.2) is over infinite time, so while it shows exactly which frequencies are present in $x(t)$, it tells nothing about when the frequencies occur. In order to extract information about both frequency and time, Gabor proposed using a window function to focus on specific time intervals of $x(t)$ [4]. Basically, the window function is zero everywhere except on a small interval around the origin. By shifting the window function in time and multiplying it by $x(t)$, only a small segment of $x(t)$ will be nonzero. Mathematically, the windowing process is represented by 2.3, where $w(t)$ is the window function and τ is the time shift.

$$x(t)w(t-\tau) \tag{2.3}$$

Figure 2.1 shows the result of windowing a signal. In the top diagram, the window has been shifted to $\tau = 1.5$ seconds. The middle diagram shows an 8 Hz sine wave and the bottom diagram shows the windowed signal; it is the result of multiplying the window and the sine wave. Only a small segment of the windowed signal is nonzero, so the Fourier Transform of this signal will give the frequency information near 1.5 seconds.

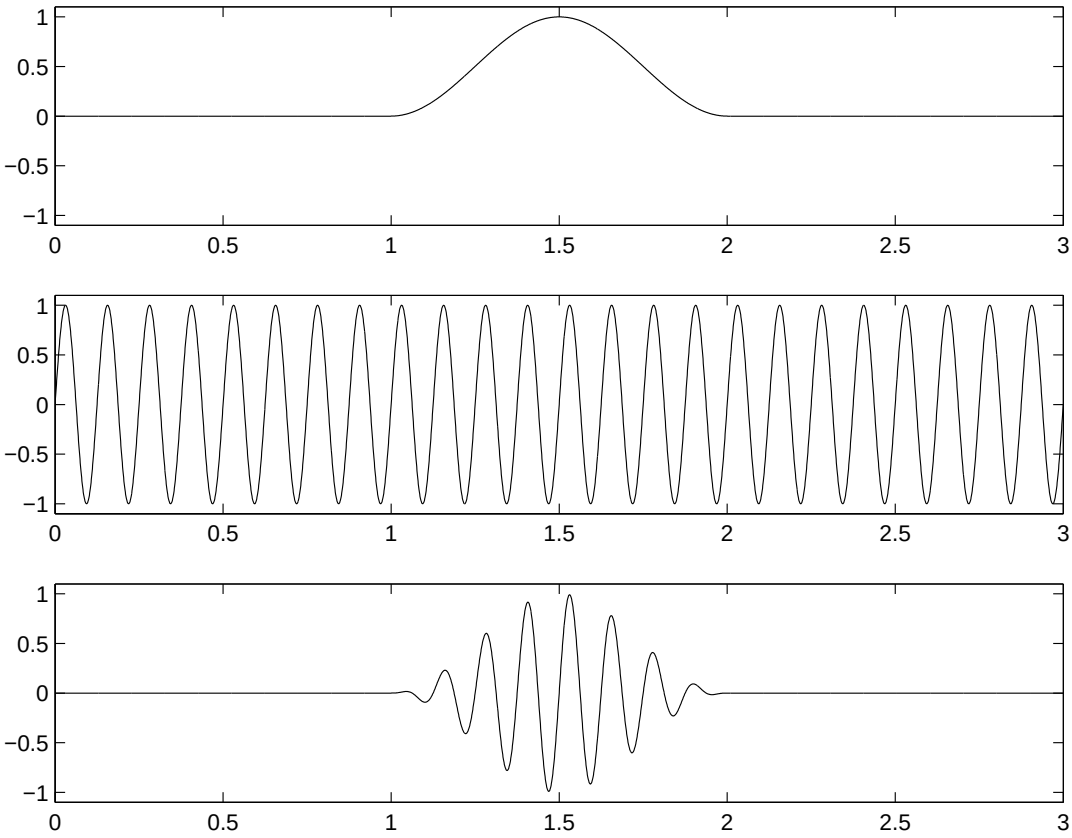

Figure 2.1: A signal is multiplied by a window function. From top to bottom: the window function, the signal, the signal multiplied by the window function.

Plugging the product in 2.3 into the equation for the Fourier Transform (2.2) gives the equation for the Short-Time Fourier Transform (STFT) (2.4).

$$X_{STFT}(\tau, \omega) = \int x(t)w(t-\tau)e^{-i\omega t}dt \tag{2.4}$$

The Fourier Transform of a product of two functions results in the convolution of the Fourier Transforms of the two functions. The consequences of this will be shown in detail later, but essentially, the duration and shape of the window affect the representation created by the STFT because the spectrum of the window is convolved with the spectrum of the signal.

A commonly used window in audio signal processing is the Hamming window, shown in Figure 2.2. It is the raised cosine defined by (2.5) with t running from 0 to 1 [5]. This equation only defines the nonzero part of the window function; the function is assumed to be zero everywhere else.

$$w(t) = 0.54 - 0.46\cos(2\pi t) \tag{2.5}$$

There is another way to look at the STFT in (2.4). Let $\Omega_{\tau,\omega}(t) = \overline{w(t-\tau)}e^{i\omega t}$.[2] Then (2.4) can be seen as the inner product of $x(t)$ and $\Omega_{\tau,\omega}(t)$ (2.6). Therefore, $\Omega_{\tau,\omega}(t)$ is a basis for the space of functions that can represent both time τ and frequency ω.

[2]A note on notation: For those who are unfamiliar or uncomfortable with functions that have variables and subscripts ($\Omega_{\tau,\omega}(t)$), let me explain. If we set $\tau = 1$ and $\omega = 2$, then $\Omega_{1,2}(t)$ represents a function of time, just as the typical $f(t)$ and $x(t)$ represent functions of time. Similarly, if we set $\tau = 2$ and $\omega = 3$, then $\Omega_{2,3}(t)$ also represents a function of time, though different from $\Omega_{1,2}(t)$. Naming both functions with an Ω tells us that they belong to a family of functions because they are related in some way (they have the same form). The subscripts τ and ω are variables used to specify unique members of the family and the t is the time variable since every function in this family is a function of time. The same function could be written as $\Omega(t, \tau, \omega)$ since τ and ω are variables, but that looks like a single function Ω with three equally important variables. It does not convey the same sense that Ω is a family of functions of time.

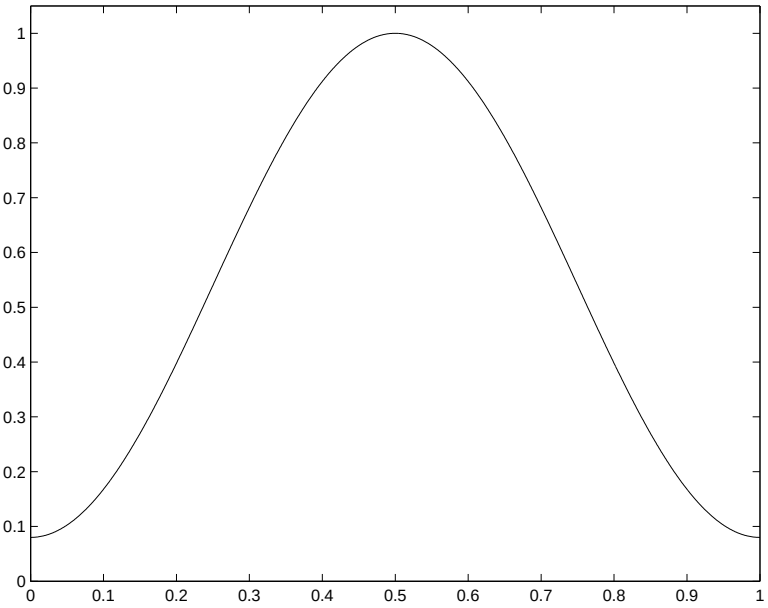

Figure 2.2: A Hamming window.

$$\begin{aligned} X_{STFT}(\tau,\omega) &= \int x(t)w(t-\tau)e^{-i\omega t}dt \\ &= \int x(t)\overline{\overline{w(t-\tau)}e^{i\omega t}}dt \\ &= \int x(t)\overline{\Omega_{\tau,\omega}(t)}dt \end{aligned} \tag{2.6}$$

In (2.4), the window function $w(t)$ does not depend on frequency. In other words, the same window function is used to evaluate every frequency. Since the window function does not change with frequency, the frequency resolution of the STFT does not change with frequency. This also implies that the time resolution does not change with frequency. Therefore, the choice of a window function determines both the frequency resolution and the time resolution for the entire representation.

The frequency of a pure tone is inversely related to the period of the waveform. A single period of a pure tone completely describes its shape for all time, so a pure tone at 10 Hz is described in 1/10 of a second and a pure tone at 1000

Hz is described in 1/1000 of a second. Therefore, it takes longer to describe low frequencies than it takes to describe high frequencies. This relates to the length of the window function in the STFT because short windows might not be long enough to capture a full period of low frequencies. If a longer window is used, it becomes difficult to locate when a high frequency occurred.

These difficulties suggest varying the window size with frequency. Long duration windows can be used to capture low frequencies and short duration windows can be used to capture high frequencies. Since the frequency resolution changes over the representation, the time resolution also changes; high frequencies will be more localized in time than low frequencies. This idea is the fundamental difference between the Short-Time Fourier Transform and the Wavelet Transform.

2.3 Wavelet Transform

The Wavelet Transform makes the window length inversely proportional to the frequency [6]. In other words, low frequencies are analyzed with long windows and high frequencies are analyzed with short windows. This is often termed a *multiresolution*, since the frequency resolution and the time resolution change over the representation. Although the idea of analyzing signals at different resolutions has existed since the beginning of the century, it was only recently that Grossman, Meyer, and Morlet created a general multiresolution theory known as Wavelet Theory [7].

The Wavelet Transform uses a set of basis functions obtained by dilations, contractions, and shifts of a unique function called the "wavelet prototype." The effect of scaling the wavelet prototype is similar to changing the size of window in the STFT. Shifting the wavelet in time is the same as shifting the window in the STFT. If the input signal $x(t)$ is continuous and the time and scale parameters are continuous, the transform is called the Continuous Wavelet

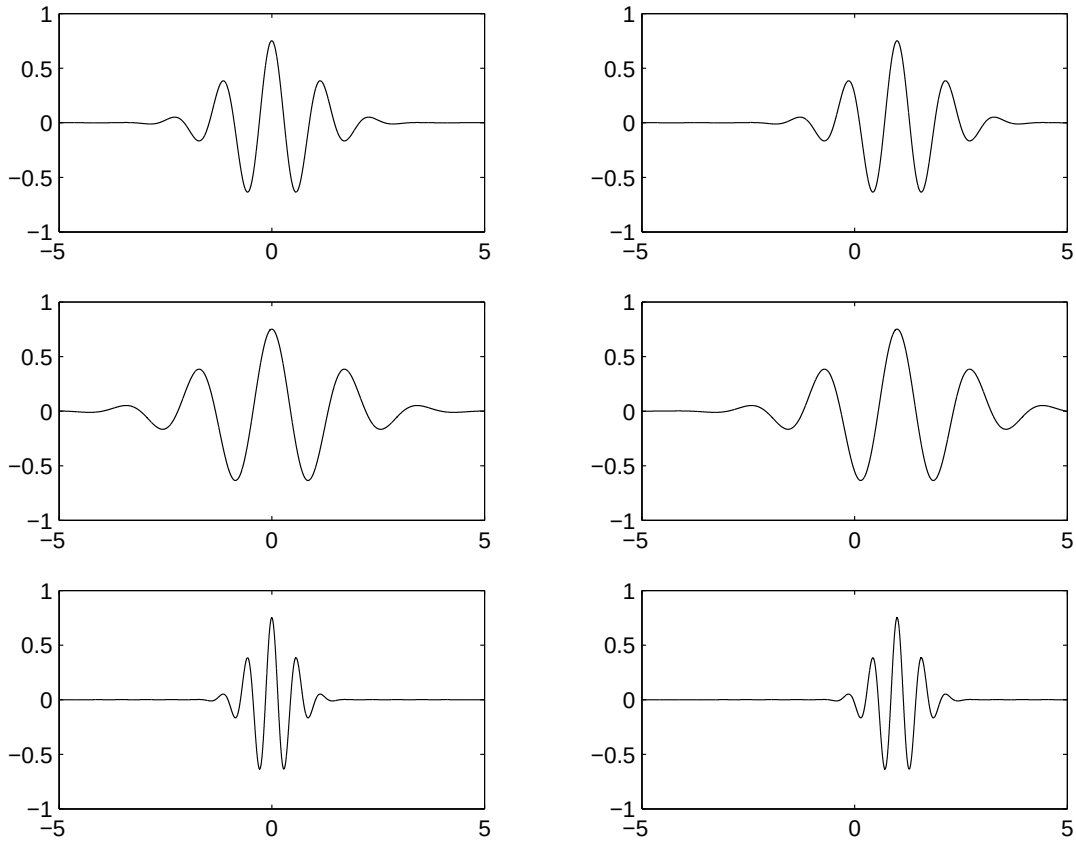

Figure 2.3: Shifted and scaled wavelets. By column, the wavelets are either shifted by 0 seconds or 1 second. By row, the wavelets are either scaled by a factor of 1, 1.5, or 0.5.

Transform (CWT).

Given an input signal $x(t)$, the CWT can be defined as (2.7), where a represents the scaling factor and b represents the time shift [8].

$$X_{CWT}(a,b) = \frac{1}{\sqrt{|a|}} \int x(t) \overline{\Psi\left(\frac{t-b}{a}\right)} dt \tag{2.7}$$

Figure 2.3 shows shifted and scaled versions of a "wavelet prototype." In the upper left, $a = 1$ and $b = 0$, so this wavelet is neither shifted nor scaled; it is the wavelet prototype. The other wavelets are shifted (by column: $b = 0$ or $b = 1$) and scaled (by row: $a = 1$, $a = 1.5$, or $a = 0.5$) versions of it.

Equation 2.7 can also be written as an inner product of $x(t)$ with the basis

function $\Psi_{a,b}(t)$. This makes the similarity between the STFT in (2.6) and the CWT in (2.8) clear. The STFT is an inner product of $x(t)$ with $\Omega_{\tau,\omega}(t)$ and the CWT is an inner product of $x(t)$ with $\Psi_{a,b}(t)$. The differences between the two transforms come directly from the differences between the two families of basis functions. This will be covered in detail in the next section.

$$X_{CWT}(a,b) = \int x(t)\overline{\Psi_{a,b}(t)}dt \tag{2.8}$$

where

$$\Psi_{a,b}(t) = \frac{1}{\sqrt{|a|}}\Psi\left(\frac{t-b}{a}\right) \tag{2.9}$$

In (2.9), as a becomes large, the basis function $\Psi_{a,b}(t)$ stretches and is able to analyze the low-frequency components of the signal. As a becomes small, the basis function $\Psi_{a,b}(t)$ contracts and is able to analyze the high frequency components of the signal. The factor $1/\sqrt{|a|}$ in (2.9) and (2.7) guarantees energy normalization [9].

The Morlet wavelet, shown in Figure 2.4, is commonly used for analyzing audio signals. It is a Gaussian modulated complex sinusoid described by (2.10) [8, 10]. The Morlet wavelet is complex valued; the figure shows the real and imaginary parts separately as solid and dashed lines.

$$\Psi(t) = \pi^{-1/4}\left(e^{-i\omega_0 t} - e^{-\omega_0^2/2}\right)e^{-t^2/2} \tag{2.10}$$

with

$$\omega_0 = \pi\sqrt{\frac{2}{\ln 2}} \approx 5.3364 \tag{2.11}$$

2.4 A Comparison of Two Time-Frequency Transforms

Now that I have introduced the basic concepts and mathematics behind the STFT and the CWT, I will apply both transforms to the same audio signals and compare the different time-frequency representations.

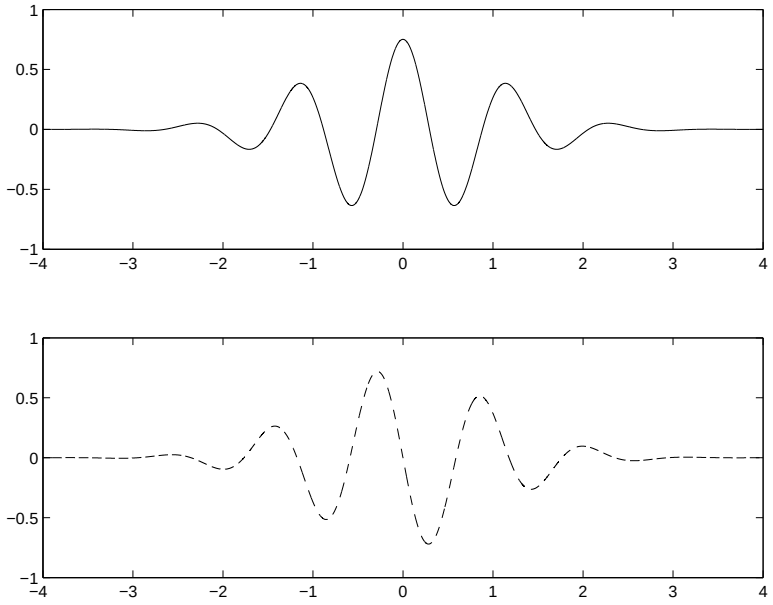

Figure 2.4: The Morlet wavelet. The real part is shown as a solid line and the imaginary part is shown as a dashed line.

2.4.1 The Signals

Music notation for the audio signals is shown in Figure 2.5. The signals were synthesized using *Csound* [11] and then analyzed with the STFT and CWT. Synthesized signals were chosen in this experiment so that the data extracted from the time-frequency representations could be compared to the data used to create the signals.

The synthesized instrument sound consisted of three harmonics with amplitudes set to 1, 0.8, and 0.6 and a linear envelope with a 50 ms rise time and 50 ms decay. The signals were synthesized at a sampling rate of 12 kHz and cropped to a length of 32768 samples (2.73 seconds). The chosen sample rate is more than adequate because the highest harmonic in any of the signals is 2095.41 Hz. The tempo was set to 120 quarter notes per minute making each quarter note 500 ms, each eighth note 250 ms, and each sixteenth note 125 ms.

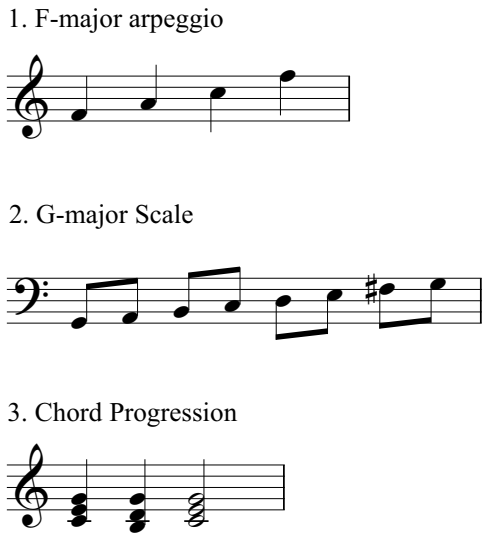

Figure 2.5: Music notation for the test signals. The F-major arpeggio, G-major scale, and chord progression were synthesized in *Csound*.

2.4.2 Analysis Techniques

The time-frequency representations of the audio signals were computed in MATLAB with an optimized version of the *Time-Frequency Toolbox for Matlab* [12]. All the time-frequency plots show time in seconds on the horizontal axis and frequency in Hertz on the vertical axis. Amplitude in decibels is shown by the darkness of the pixels from white to black.

To compare the time-frequency representations, I developed specialized MATLAB functions to measure the center frequency, frequency width, start time, and duration of the harmonics. Figure 2.6 shows how these values were calculated for this experiment. For center frequency, I used parabolic interpolation in the frequency domain (Appendix B describes this technique in detail). I measured frequency width by finding the interval, or ratio, between the frequencies of the two points that were 3 dB down in amplitude from the amplitude of the center frequency.

The start time of a harmonic was calculated by searching for a strong rise

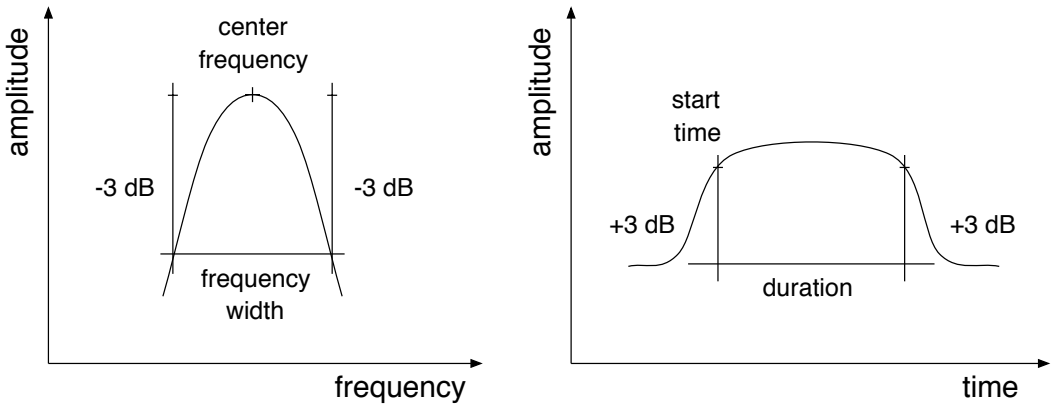

Figure 2.6: The calculation of center frequency, frequency width, start time, and duration.

in the time-domain representation. The data had been thresholded, so there was a non-zero floor at about -26 dB. The point in time when the amplitude reached 3 dB up from the floor was taken as the start time. The length of time between this point and the last point that was 3 dB above the floor became the duration.

The value 3 and the techniques for determining the parameters were designed specifically for this experiment. They were robust, simple to implement, and returned consistent data; they clearly showed the differences between the STFT and the CWT.

I chose the parameters of the STFT and CWT so that both transforms produced the same frequency width around the fundamental of the lowest frequency in the signals, G at 98 Hz. This choice was arbitrary because I could have fixed the width at any frequency. I chose to set the width to be the same for low frequencies so that the differences between the transforms for high frequencies could be observed.

For the STFT, I used an FFT size of 8192, a window size of 5601, and a step size of 128. This is an abnormally large window size, but it was necessary

to make the STFT have the same frequency width around 98 Hz as the CWT. This, of course, greatly affects the time resolution of the transform, but I was more interested in the trends of the data gathered from the representations than the actual values.

The step size determined the number of columns in the time-frequency representation. Since the signals were all 32768 samples long, the resulting representations had 256 columns. There were 8192 rows, so the size of the STFT representation was 2,097,152 complex values. I converted the complex-valued data into magnitudes for simplicity.

I calculated the CWT from 12 Hz to 6000 Hz (0.001 to 0.5 in normalized frequency) at 512 logarithmically spaced frequencies. The 'wave' parameter—which corresponds to half length of the Morlet wavelet at coarsest scale—was set to 70. The step size was set to 128 to make the CWT representation have the same number of columns as the STFT representation. The total size was much smaller, however, 131,072 complex values or one sixteenth (6.25%) of the size of the STFT matrix. As in the STFT, the complex-values were converted to magnitudes.

The time-frequency representations were thresholded by 5%. In other words, any point less than 5% of the maximum value of the matrix was set to 5% of the maximum value, creating a non-zero floor for the matrix. The magnitudes were then converted to dB ($20 \log_{10}(x)$).

2.4.3 Results

Figure 2.7 shows the STFT and the CWT of the F-major arpeggio. The frequency axis has been scaled to show detail between 300 and 2200 Hz. Looking at the STFT representation, we can see that the frequency resolution is precise because the harmonics of each note are shown as thin lines. This precision is due to the large window size. The window size, however, affects the time resolution

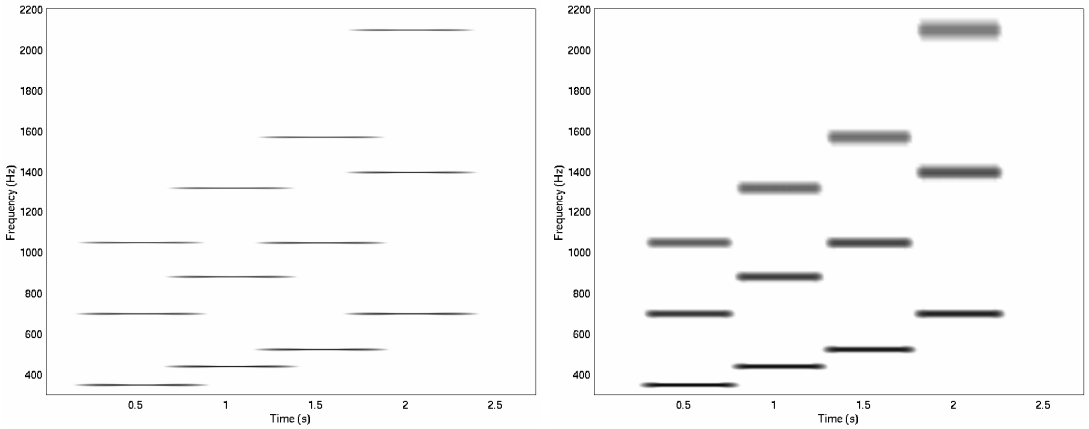

(a) STFT of the arpeggio

(b) CWT of the arpeggio

Figure 2.7: The time-frequency representations of signal 1, the F-major arpeggio.

and all the harmonics in the plot are equally overlapped by approximately 25%.

The harmonics in Figure 2.7(b) are represented by thicker lines than those in Figure 2.7(a), so the frequency width of the CWT is not as precise as that of the STFT. The higher harmonics are also thicker than the lower harmonics. The loss of frequency resolution for high frequencies results in a gain of time resolution and therefore, the amount of overlap decreases as frequency increases.

Figure 2.8 shows the STFT and CWT of signal 2, the G-major scale. The frequency axis has been scaled to show detail between 50 and 600 Hz. In the STFT representation, the harmonics are clearly resolved in frequency but are overlapped in time. As with the STFT of the arpeggio, the thickness of the harmonics (frequency width) and the amount of overlap appear to be the same for all harmonics. This suggests that the frequency and time resolution are constant for the plot.

For low frequencies, the harmonics in CWT representation appear long in duration, thin in frequency width, and overlapped by approximately 50%. For

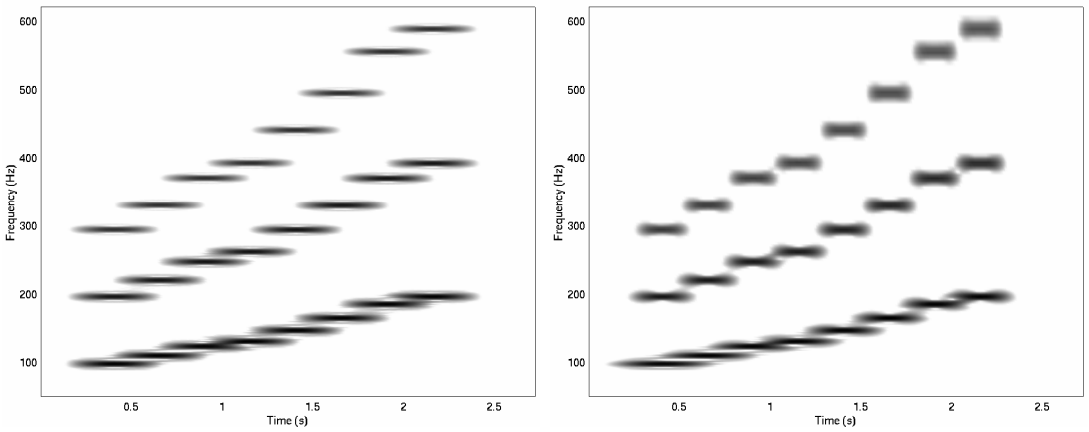

(a) STFT of the scale

(b) CWT of the scale

Figure 2.8: The time-frequency representations of signal 2, the G-major scale.

high frequencies, the harmonics appear thick in frequency width, short in duration, and separated in time. Therefore, frequency and time resolution vary over the plot.

Figure 2.9 shows the STFT and CWT of signal 3, the chord progression. The observations of constant time-frequency resolution for the STFT and varying time-frequency resolution for the CWT hold for these representations.

The observed differences between the two time-frequency representations were quantified using the frequency-domain and time-domain algorithms described in Section 2.4.2. In MATLAB, the frequency-domain is represented as columns, so a single column will show the amplitudes of different frequencies at a fixed point in time. The time-domain is represented as rows, so a single row will show how the amplitude of a particular frequency varies over time.

Table 2.1 shows the frequency data from the STFT and CWT of signal 2, the G-major scale. Columns 1–3 show the note names, harmonic numbers, and actual frequencies for each harmonic of each note. Columns 4–5 show the difference, or error, between the calculated frequency and the actual frequency.

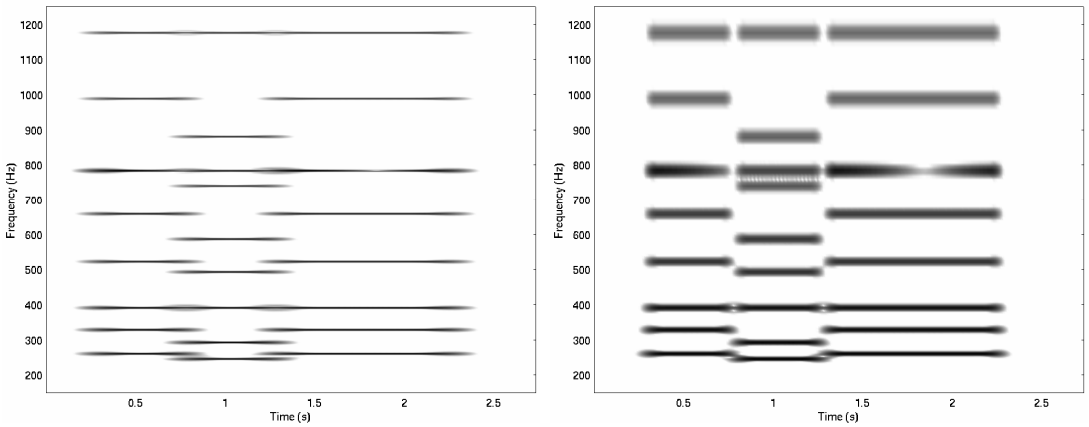

(a) STFT of the chord progression

(b) CWT of the chord progression

Figure 2.9: The time-frequency representations of signal 3, the chord progression.

Columns 6–7 show the calculated frequency width. All the values in the table are in cents (100 cents is a semitone).

The center frequencies calculated from the STFT representation get closer to the actual frequencies as frequency increases because the error, in cents, decreases. For the CWT, the error is almost constant, at 20 cents, over the entire range of frequencies. Figure 2.10(a) shows the center frequency error for both transforms over frequency. Quantified data from all three test signals was used to generate the figure and a single outlier was removed.

The frequency width extracted from both representations initially decreases as frequency increases. Above 500 Hz, the frequency width of the CWT is close to constant while the frequency width of the STFT continues to decrease. This relationship is shown in Figure 2.10(b). Data from all three signals was used to generate the figure.

Table 2.2 shows the quantified time data from the STFT and CWT of the G-major scale. Columns 1–3 show the note names, harmonic numbers, and actual start times for each harmonic of each note. Columns 4–5 show the

Note Name	Harm Num	Freq (Hz)	STFT Freq Error	CWT Freq Error	STFT Freq Width	CWT Freq Width
G	1	98.00	25.45	21.09	78.29	78.28
	2	196.00	12.87	20.92	40.74	53.36
	3	294.00	8.54	20.97	27.74	47.21
A	1	110.00	22.52	20.81	65.14	66.92
	2	220.00	11.45	20.88	36.14	49.50
	3	330.00	7.64	20.96	24.36	46.46
B	1	123.47	20.62	20.48	65.19	68.16
	2	246.94	9.92	20.76	33.90	49.47
	3	370.41	6.80	20.99	21.29	44.64
C	1	130.81	11.97	14.72	59.80	62.17
	2	261.63	8.87	20.42	32.06	46.53
	3	392.44	6.39	20.92	19.81	42.00
D	1	146.83	16.28	19.90	54.83	58.92
	2	293.66	8.68	21.01	28.16	46.08
	3	440.50	5.74	20.99	18.52	42.13
E	1	164.81	15.23	20.64	50.41	57.75
	2	329.63	7.61	21.00	23.42	44.59
	3	494.44	5.10	20.91	16.76	40.48
F ♯	1	185.00	14.28	21.23	43.51	51.90
	2	369.99	6.84	21.00	22.33	43.80
	3	554.99	4.57	21.02	14.17	40.26
G	1	196.00	14.88	23.01	38.66	53.44
	2	392.00	6.54	21.09	21.12	43.70
	3	587.99	4.25	20.97	14.15	41.77

Table 2.1: Frequency error and width table (in cents) for the STFT and CWT of signal 2.

calculated start times in the harmonics in the STFT and CWT. Columns 6–7 show the calculated durations of the harmonics in the STFT and CWT. The actual duration of all the harmonics is 250 ms because the scale was played as eighth notes at 120 beats per minute.

The start times of the harmonics in the STFT representation are far from the actual start times; the mean difference between the calculated time and actual time is 109.69 ms. The large start time error is directly caused by the window size used in the experiment. The error initially decreases and then becomes almost constant.

The start times of the harmonics in the CWT, however, get closer to the

Note Name	Harm Num	Start Time	STFT Start Time	CWT Start Time	STFT Duration	CWT Duration
G	1	280	160.28	122.10	518.85	594.69
	2	280	169.61	234.12	491.32	362.73
	3	280	183.82	272.45	465.64	288.06
A	1	530	401.34	380.44	516.92	554.98
	2	530	420.03	496.31	489.86	339.96
	3	530	433.17	528.24	465.54	275.80
B	1	780	658.45	665.06	505.92	529.56
	2	780	671.76	754.21	490.49	326.80
	3	780	683.65	782.67	463.72	268.41
C	1	1030	911.07	718.19	513.57	694.45
	2	1030	921.98	1008.41	487.99	316.30
	3	1030	933.34	1030.29	465.19	265.79
D	1	1280	1162.29	1195.92	508.14	444.54
	2	1280	1171.34	1265.15	489.69	302.92
	3	1280	1184.55	1289.09	461.90	253.13
E	1	1530	1411.58	1458.86	508.52	414.96
	2	1530	1419.08	1520.92	492.28	290.18
	3	1530	1435.90	1542.89	460.74	246.01
F ♯	1	1780	1662.03	1723.10	503.75	386.61
	2	1780	1670.49	1775.54	489.16	282.84
	3	1780	1683.54	1795.84	462.61	239.53
G	1	2030	1881.44	1966.09	540.00	387.34
	2	2030	1921.75	2023.81	488.94	278.87
	3	2030	1934.91	2044.57	461.13	240.82

Table 2.2: Start time and duration table (in milliseconds) for the STFT and CWT of signal 2.

actual start time as frequency increases. Figure 2.11(a) shows the start time error of the STFT and CWT over frequency. Data from all three signals was used to generate the figure.

The duration data shows the same trend as the start time data. For the STFT, the mean duration of a harmonic is 489.24 ms with a standard deviation of 22.32 ms. This difference initially decreases then becomes approximately constant after 700 Hz. The durations of the harmonics calculated from the CWT get closer to the actual durations as frequency increases. Figure 2.11(b) shows the duration error of the STFT and CWT over frequency. Data from all three signals was used to generate the figure.

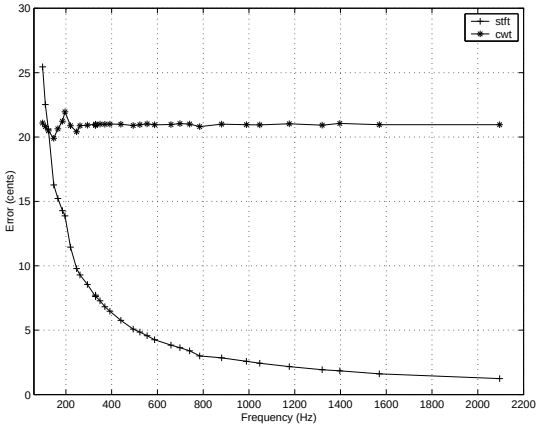

(a) The center frequency estimation error over frequency.

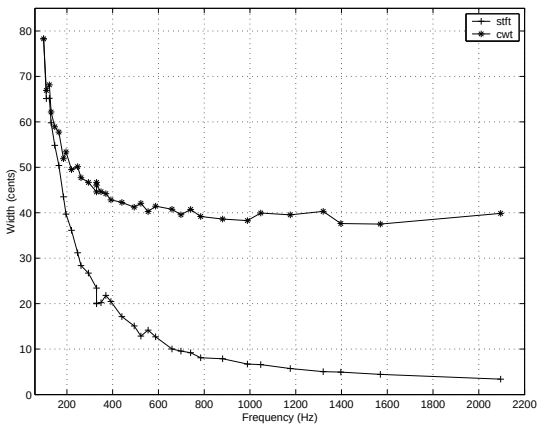

(b) The frequency width over frequency

Figure 2.10: The center frequency estimation error and estimated frequency width in cents for the STFT and CWT.

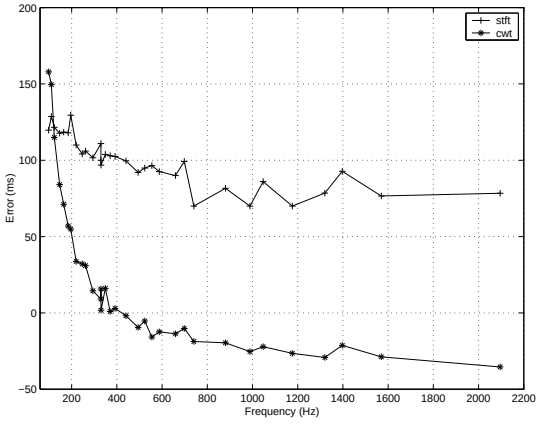

(a) The start time estimation error over frequency.

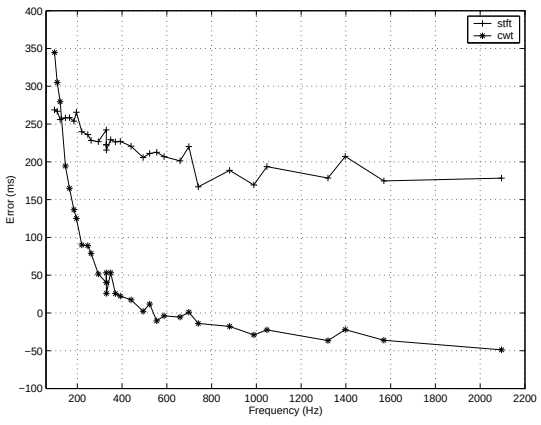

(b) The duration estimation error over frequency

Figure 2.11: The start time and duration estimation errors for the STFT and CWT.

2.4.4 Conclusions

The Short-Time Fourier Transform and the Continuous Wavelet Transform were applied to the same audio signals and the resulting time-frequency representations were compared. The results above display the important difference between the two transforms. If the frequency resolution is fixed at a particular frequency for both transforms, the CWT will have better time resolution above that frequency and better frequency resolution below that frequency than the STFT. Of course, this improvement comes at the expense of the frequency resolution for high frequencies and the time resolution for low frequencies. In other words, the time resolution is fixed for the STFT and variable for the CWT.

A potential advantage of the CWT is the size of the time-frequency representation. For the signals above, the CWT produced representations with 131,072 complex numbers. The STFT produced representations with 2,097,152 complex numbers. In other words, an STFT with the same low frequency response as a CWT will produce a representation sixteen times larger than the representation produced by the CWT.

The STFT has two significant advantages over the CWT. Since the time resolution is fixed over the entire frequency range, synchrony in the onsets of harmonics can be detected. This is important for determining if harmonics belong to a particular sound; common onsets suggest that harmonics belong together.

The other advantage is computational speed. The FFT, and therefore the STFT, is an optimized and efficient algorithm. On most computers, the STFT of a signal can be quickly calculated. The CWT, however, relies on convolutions and is an order of magnitude less efficient than the STFT. Computing the convolutions in the frequency domain speeds up the CWT dramatically, but it still cannot compete with the STFT. In practice, dyadic Discrete Wavelet

Transforms are often used to create time-scale representations because there are fast algorithms available. Extracting time and frequency information from these representations is a possibility for further study.

3 Analysis/Synthesis Systems

The last chapter focused primarily on using time-frequency transforms for signal analysis. Analysis can reveal the details of a sound, but it does not tell if those details are perceptible. This is why sound synthesis techniques are often used when analyzing sounds; one way to determine the quality of the analysis data is to synthesize a sound from it and compare that sound to the original. The similarities and differences tell what the analysis technique can and cannot represent.

Not all analysis techniques provide enough information for synthesis. For example, it would be impossible to reconstruct a signal from its mean and variance. The advantage of the two transforms described in Chapter 2 is that they are invertible. In other words, inverse transforms can convert the time-frequency representations back into time-domain signals. This makes the STFT and CWT perfect for sound analysis and synthesis.

Sound analysis/synthesis systems are used for more than just determining the differences between two sounds. They are also powerful tools for electronic music composition. Manipulating the analysis data prior to synthesis can create various timbral effects, time scaling, or pitch shifting. Analysis data from different sound sources can also be combined to achieve cross-synthesis or morphing effects.

The STFT is the transform used in most analysis/synthesis systems, but many of them have needed additional algorithms to be able to represent both the harmonic and the noise components of sounds. It is likely that the STFT is chosen out of convenience—it is well documented and there is an efficient algorithm for calculating it—not because it provides a better model for representing sound. Although all the analysis/synthesis systems described in this chapter use

Figure 3.1: The phase vocoder analyzes a sound, modifies the analysis data, and synthesizes the sound.

the STFT, their designs can be extended to use any invertible time-frequency transform. In the Spectral Modeling Toolbox, described in Chapter 4, there are two time-frequency transforms available.

The next sections cover the sound analysis/synthesis techniques that influenced the design of the Spectral Modeling Toolbox. The three systems described below do not represent a comprehensive list of analysis/synthesis systems and their descriptions only cover their important features; the cited references should be used to learn more about the details of these systems.

3.1 The Phase Vocoder

The phase vocoder is widely used for time scaling and pitch shifting and the ideas behind its design can be found in all the analysis/synthesis systems that follow. Essentially, the phase vocoder uses a Short-Time Fourier Transform (STFT) for analysis and an Inverse Short-Time Fourier Transform (ISTFT) for synthesis. Time scaling and pitch shifting are achieved by modifying the analysis data prior to synthesis [13].

On a conceptual level, the phase vocoder is the system shown in Figure 3.1. The analysis stage uses a transform to decompose a sound onto a time-frequency basis. The result is a set of data that describes the evolution of a sound's frequency components over time.

This system assumes that the time-frequency transform is able to represent important features in the signal. In the case of the phase vocoder, the transform is the STFT, so the sound is described in terms of windowed sinusoids. The

frequencies of the sinusoids are all multiples of F_s/N, where F_s is the sampling frequency and N is the DFT size. In other words, the phase vocoder considers all frequency samples of the DFT to be equally important and a sound is synthesized using the data for all N sinusoids between 0 and $F_s/2$ Hz.

A sine wave model is appropriate for many sounds, especially those with steady harmonic components. Therefore, the phase vocoder will be able to analyze, modify, and synthesize such sounds with accuracy. Sounds with transient and noise components, however, are not easily represented by sine waves and the phase vocoder will have difficulty representing these sounds.

The classic phase vocoder is typically used to time scale and pitch shift sounds. To scale time, the time trajectories of the frequency components are interpolated before synthesis. To shift pitch, the sound is first time-scaled and then sample-rate converted to be the same duration as the original sound [13]. While time scaling and pitch shifting are the most common modifications, many other possibilities have been designed and implemented by Christopher Penrose in his PVNation software [14] and Eric Lyon in his PowerPV software [15].

The major problem with the phase vocoder as an analysis/synthesis system is that the analysis stage does not reveal information specific to the sound being analyzed; all sounds are represented by N time-varying sinusoids. Clearly, many of those sinusoids are not necessary to characterize most sounds. For example, harmonic sounds can be modeled using only sinusoids at integer multiples of a fundamental frequency. McAulay and Quatieri extended the phase vocoder to address this problem.

3.2 The McAulay-Quatieri Analysis/Synthesis Technique

Instead of using all N frequency samples per frame, the McAulay-Quatieri (MQ) analysis/synthesis technique isolates peaks in the spectrum since they represent regions of high energy. Figure 3.2(a) shows the peaks of a simple

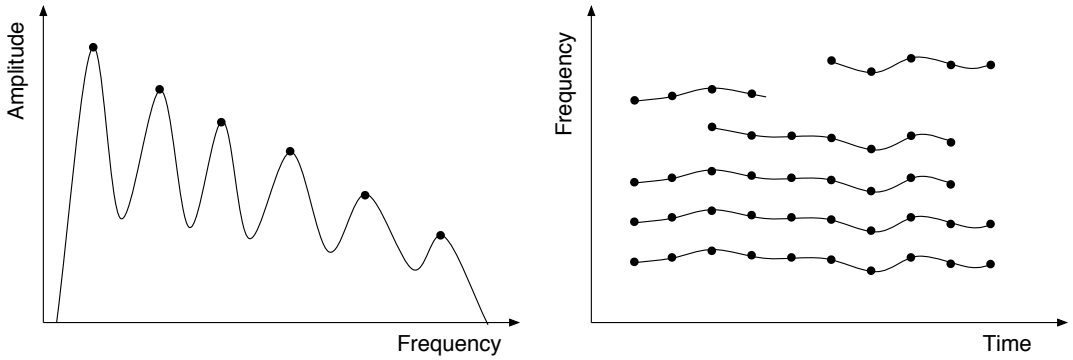

(a) Detecting peaks

(b) Forming sinusoid tracks

Figure 3.2: The McAulay-Quatieri analysis/synthesis technique forms sinusoid tracks by connecting the peaks of each frame of the STFT.

frequency spectrum. If the DFT size is 1024 (1024 frequency samples) for this frame, then there is a significant amount of data reduction by storing only 6 of the 1024 points. Reducing the amount of analysis data provides a simpler description of a sound and facilitates its manipulation.

The justification for reducing a complete frequency spectrum to its peaks comes from the psychoacoustic phenomenon of masking. If two sounds are close together in frequency, one will mask, or interfere with, the perception of the other. Generally speaking, a loud sound will inhibit the perception of softer sounds above it in frequency [1, p. 315]. Since peaks in a frame of the STFT represent regions of high energy, they will mask the perception of nearby softer frequencies.

For every frame of the STFT, the MQ technique locates the peaks and forms tracks of peaks by connecting peaks in the current frame to nearby peaks in the previous frame. A new track begins when there is no peak in the previous frame that is close in frequency to a peak in the current frame. A track ends when there is no peak in the current frame that is close enough to it in frequency.

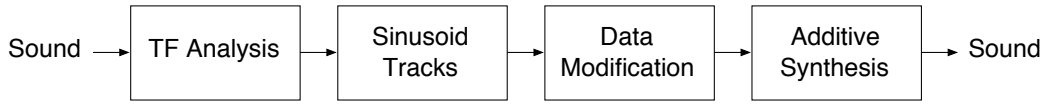

Figure 3.3: The McAulay-Quatieri analysis/synthesis system extends the phase vocoder by extracting sinusoid tracks from the time-frequency analysis data.

Figure 3.2(b) illustrates the formation of sinusoid tracks from peaks in the frames of the STFT.

Since the information in the STFT has been reduced to sinusoid tracks, the MQ technique resynthesizes the sound using additive synthesis. The frequency and amplitude data of the sinusoid tracks control a bank of oscillators to produce sound. Similar to the phase vocoder, the analysis data can be modified before synthesis to time scale or to pitch shift the sound, as well as to produce various timbral effects.

The MQ system is shown in Figure 3.3. It is similar to the phase vocoder except that the TF Synthesis stage has been replaced with Additive Synthesis and the analysis data is reduced to Sinusoid Tracks. The advantage of the MQ technique over the phase vocoder is that the analysis data represents salient features of the sound. The major disadvantage of the MQ technique is that, like the phase vocoder, it is built upon a sine wave model. This means it will have the same problems representing sounds with noise and transient components. The Spectral Modeling Synthesis (SMS) technique addresses this problem by including noise in its sound model.

3.3 Spectral Modeling Synthesis

At about the same time as McAulay and Quatieri developed their analysis/synthesis technique, Julius Smith III and Xavier Serra at CCRMA developed another STFT peak-tracking technique called PARSHL. PARSHL differed

from MQ in that interpolation on the spectral peaks was used for greater accuracy and different algorithms were used for determining the beginnings and the endings of the sinusoid tracks [16]. Essentially, both techniques solved the problem of extracting sinusoid tracks from the STFT and they both relied on a sine wave model of sound.

Serra and Smith extended PARSHL to represent noise components in signals and called the new system Spectral Modeling Synthesis (SMS). Unlike the phase vocoder and MQ, SMS uses more than a sine wave model of sound. The model is called deterministic plus stochastic where the deterministic part models the sine wave components and the stochastic part models the noise components. Mathematically, the input sound $s(t)$ is modeled as the sum of R sine waves plus the noise signal $e(t)$. This is shown in equation 3.1 [16]. The functions $A_r(t)$ and $\theta_r(t)$ are the amplitude and frequency trajectories of each sine wave.

$$s(t) = \sum_{r=1}^{R} A_r(t) \cos[\theta_r(t)] + e(t) \tag{3.1}$$

The stochastic component, or residual, can be determined by subtracting the synthesized sound from the original sound [16]. This is possible because the phases of the sinusoids are preserved. After subtraction, the stochastic component is modeled with filtered white noise where the shape of the filter is determined by fitting a curve to the magnitude spectrum of the residual. An overview of SMS is shown in Figure 3.4

Preserving the phase information also allows SMS to use an inverse STFT to synthesize the deterministic component. The magnitude and phase values for each peak are placed in a spectral buffer and then the inverse transform is computed. The filtered white noise is then added to complete the synthesis.

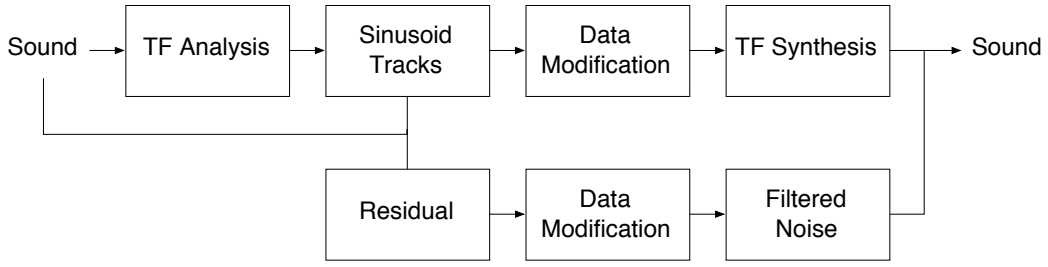

Figure 3.4: Spectral Modeling Synthesis can model noise and transients with a residual signal.

While representing sound as sine waves plus noise greatly improves the quality of the synthesis, it also demonstrates that a pure sine wave model is inadequate for many sounds. Sound, in general, cannot be reduced to a discrete number of sine waves and this suggests that analysis/synthesis systems should not be limited to the sine wave basis of the STFT. In chapter 2, the CWT was introduced as a transform that models sound using a different basis. The Spectral Modeling Toolbox takes a generalized approach by allowing several time-frequency transforms to be used, including the STFT and the CWT.

3.4 Design of the Spectral Modeling Toolbox

The Spectral Modeling Toolbox extends the ideas of MQ and SMS to work with other time-frequency transforms. In addition, the framework of the Toolbox is flexible, so many analysis/synthesis systems can be created using its functions. Although the overall design descends from MQ and SMS, the implementation differs significantly to allow the user to control any aspect of the system. A global view of the system is shown in Figure 3.5. This rest of this chapter will give detailed descriptions of each part of the system.

3.4.1 TF Analysis

The two functions used for time-frequency analysis were discussed in detail in Chapter 2. Essentially, the TF analysis stage takes a sound file as input and

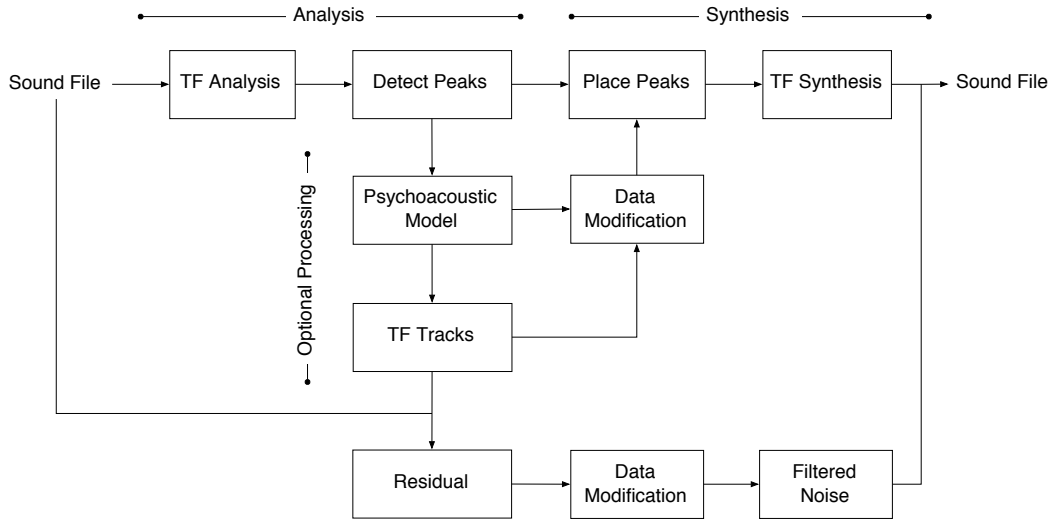

Figure 3.5: A basic overview of the Spectral Modeling Toolbox for MATLAB.

returns a time-frequency representation.

3.4.2 Detect Peaks

The peak detection stage takes the output of the TF Analysis stage and locates peaks in the representation frame by frame. For each frame, there are two steps used to calculate the peaks. The first step finds all of the places in the sampled spectrum (above a threshold), where the first derivative changes from positive to negative. The second step improves the frequency accuracy of these points using parabolic interpolation. The details of parabolic interpolation are discussed in Appendix B.

The peak detection stage returns a list of peaks for each frame with each peak containing frequency, amplitude, and phase information. Unlike MQ and SMS, the peak detection stage in the Toolbox does not include any logic for selecting prominent peaks other than the small threshold. Currently, prominent peaks are selected by the psychoacoustic model, but custom selection algorithms could be easily implemented.

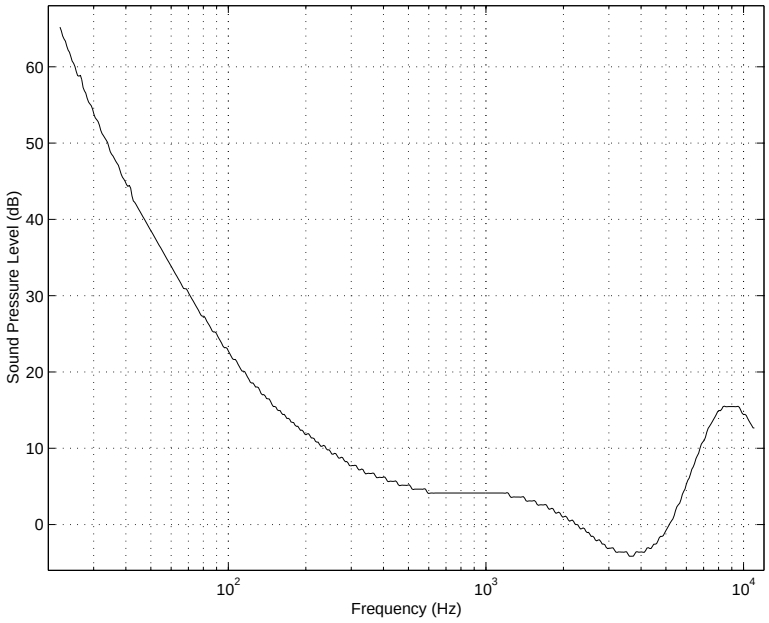

Figure 3.6: The minimum audible field curve shows that the audibility of a sound is frequency dependent [17, p. 283].

3.4.3 Psychoacoustic Model

The algorithms in the Toolbox for selecting prominent peaks are based on a psychoacoustic model. The first part of the model removes any peaks that are below the Minimum Audible Field curve shown in Figure 3.6 [17, p. 283]. The audibility of a sound is dependent on both frequency and sound pressure level (amplitude), so any peak that falls below the curve is considered inaudible and is removed from the list of peaks.

The second part of the psychoacoustic model takes into account the masking phenomenon that occurs when two sounds are close in frequency. The five curves in Figure 3.7(a) show the amount of masking caused by a 400 Hz tone at 20, 30, 40, 50, and 60 dB SPL [19]. For low levels, the 400 Hz masker only affects frequencies close to it. At 50 and 60 dB, the 400 Hz masker affects frequencies up to 600 Hz; these frequencies need to be raised in amplitude in order to be perceived.

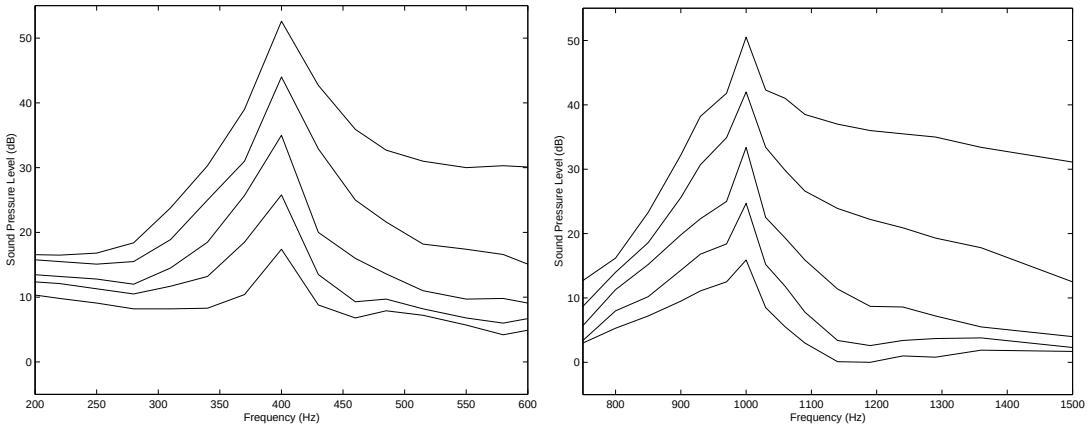

(a) Masking caused by a 400 Hz tone at different levels

(b) Masking caused by a 1000 Hz tone at different levels

Figure 3.7: The masking caused by a 400 Hz tone and a 1000 Hz tone at 20, 30, 40, 50, and 60 dB SPL [18].

Similarly, the five curves in Figure 3.7(b) show the amount of masking caused by a 1000 Hz tone at 20, 30, 40, 50, and 60 dB [19]. As with the 400 Hz masker, the amount of masking is dependent on amplitude, but it is also dependent on frequency because the curves in 3.7(b) are different from the curves in 3.7(a).

The masking algorithm in the Toolbox uses 25 masking curves obtained from psychoacoustic data. The curves are centered at 250, 400, 1000, 4000, and 6030 Hz and for each frequency there are five amplitude levels: 20, 30, 40, 50, and 60 dB. To calculate the amount of masking that occurs at an arbitrary frequency, the masking algorithm interpolates between the two closest curves.

The psychoacoustic model is not the only, or the simplest, way to determine the prominent peaks. It is optional and other algorithms—such as a frequency dependent threshold—could take its place.

3.4.4 TF Tracks

After the prominent peaks have been detected by the psychoacoustic model, they can be arranged into time-frequency tracks. This is similar to the sinusoidal

tracks in MQ and SMS.

When using other time-frequency transforms, however, the peaks do not represent sinusoidal components, so the tracks are technically not sinusoidal tracks. For example, a wavelet transform would have wavelet tracks because the basis is the set of wavelets. The track-forming concept still applies because peaks in a time-frequency representation represent points of high time-frequency energy. These points are connected into tracks to facilitate manipulation at later stages.

3.4.5 Residual

The residual stage calculates the residual signal by synthesizing the TF tracks and subtracting the synthesized signal from the original. The residual signal was discussed in the section on SMS; it reveals the parts of the input signal that are not easily represented by the model. The residual can be modeled with filtered noise or used as is. It is typically added to a synthesized signal to add realism.

3.4.6 Data Modification

As in all the analysis/synthesis systems discussed in this chapter, the analysis data can be modified before synthesis. This allows for spectral manipulation, time stretching, pitch scaling, cross synthesis, and other effects. The residual signal can also be modified to enhance attacks or reduce noise in the signal.

Essentially, the functions in this stage take a type of input and return the same type of output. A simple function, like time scaling, only needs a list of peaks; it can take the output of the peak detection stage. More advanced functions require TF tracks, so a TF track forming function needs to be run in advance.

3.4.7 Place Peaks

The place peaks stage takes a list of peaks or a set of TF tracks as input and generates a time-frequency representation. The process begins with an empty spectral buffer. The amplitude and phase values for each peak are added to the correct location in the spectral buffer. Basically, the place peaks stage does the opposite of the detect peaks stage and prepares a spectral buffer for the inverse transform.

3.4.8 TF Synthesis

The TF synthesis stage takes the spectral buffer and inverts it using an inverse time-frequency transform. This produces a time-domain signal which can be added to the residual signal to produce the final sound file.

4 The Spectral Modeling Toolbox

The end of the last chapter gave an overview of the Spectral Modeling Toolbox. This chapter will present the some of the functions in the Toolbox through code examples and diagrams. The code samples in each section assume that the variables from the previous sections are still in memory.

4.1 Installing the Toolbox

The Spectral Modeling Toolbox can be downloaded from `http://eamusic.dartmouth.edu/~kimo/smt` or `http://homepage.mac.com/kimo/smt`. Please email questions, comments, and bug reports to `kimo@mac.com`.

The Toolbox is a tarred and gzipped folder of MATLAB files. To extract these files on a UNIX platform, execute the command below. A folder named SMToolbox will be created. In that folder is a README file with the latest information and detailed installation instructions.

```
# tar -xzvf SMToolbox.tar.gz
```

To use the Toolbox, the functions need to be in your MATLAB path. Read the README file for the list of directories and how to add them to your path.

Once the Toolbox is properly installed, the command `help smt` will display the list of available functions. All the functions begin with the prefix `smt_` so that they do not conflict with functions from other toolboxes.

4.2 Reading and Writing Audio Files

The Toolbox uses MATLAB's `wavread` or `auread` functions to read audio files. The command below will read an audio file named *filename.wav* and store it in a variable named *signal*. The semicolon at the end is very important: without it, all the samples in the file will be printed to the screen.

```
>> signal = wavread('filename.wav');
```

If *filename.wav* is a mono file, the *signal* variable will be a single column vector, and if it is a stereo file, the *signal* variable will be a two column matrix. In both cases, the number of rows will be equal to the number of samples in the file.

To write audio files, use the commands `wavwrite` or `auwrite`. Typing `help` on any command will show all the available options. Below, the *signal* vector is written to a sound file *outfile.wav* with a sampling rate of 44100. On some platforms, `soundsc` will play the sound at the specified sampling rate.

```
>> help wavwrite
>> wavwrite(signal,44100,'outfile.wav');
>> soundsc(signal,44100);
```

4.3 TF Analysis and TF Synthesis

In this section, we will complete a simple analysis and synthesis of an audio file. In the SoundFiles directory, there is a recording of a saxophone called *sax.wav*. Use the `wavread` command to read the sound into the *signal* variable and the sampling rate into the *Fs* variable. Take the Short-Time Fourier Transform of the signal with hop size set to 128 samples, FFT size set to 2048 samples, and window size set to 1025 samples. The time-frequency representation is returned to the *tfr* variable and a time-frequency transform structure is returned to the *tfr_s* variable.

```
>> [signal,Fs] = wavread('sax.wav');
>> help smt_stft
>> [tfr,tfr_s] = smt_stft(signal,128,2048,1025);
```

The time-frequency transform structure holds information related to the time-frequency representation. This information is used by other functions so we will examine its contents by typing its name at the MATLAB prompt. To access any of the fields individually, type the variable name, followed by a period, followed by the field name (example `tfr_s.N`).

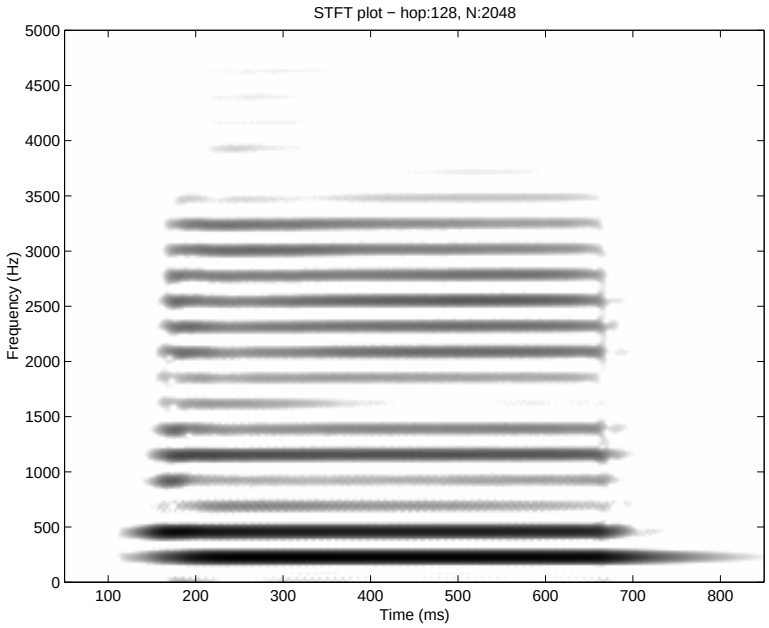

Figure 4.1: The STFT of a saxophone note scaled to show detail between 50 to 850 ms and 0 to 5000 Hz.

```
>> tfr_s
tfr_s =
        type: 'stft'
        Fs: 44100
        N: 2048
        max: 143.4354
        w: 'hamming'
        h: 1025
        hop: 128
```

The `smt_plotTFR` function takes the time-frequency representation (*tfr*) and the time-frequency transform structure (*tfr_s*) to produce a plot similar to Figure 4.1. The `axis` command scales the x-axis to show times between 50 and 850 ms and the y-axis to show frequencies between 0 and 5000 Hz.

```
>> help smt_plotTFR
>> smt_plotTFR(tfr,tfr_s)
>> axis([50 850 0 5000])
```

To resynthesize the signal, use the `smt_istft` function. The signal can then be listened to with `soundsc` or written to a file with `wavwrite`. The `smt_istft` function normalizes the signal, so it may be louder than the original.

```
>> help smt_istft
>> outSignal = smt_istft(tfr,tfr_s);
>> soundsc(outSignal,44100);
>> wavwrite(outSignal,44100,'outSignal.wav');
```

Before moving on, it is important to understand the format of the time-frequency representation returned from the `smt_stft` function. The `whos` command shows all of the current variables (and their sizes), and the `size` command shows the size of a particular variable.

```
>> whos
>> size(tfr)
ans =
    2048    337
```

This time-frequency representation has 2048 rows and 337 columns. The data is complex valued, so the `abs` and `angle` functions should be used to convert the data to magnitude and phase values. In this thesis, I have been referring to the columns of time-frequency representations as frames.

The commands below will plot the frequency content of the 100^{th} frame as shown in Figure 4.2. Typing `tfr(:,100)` tells MATLAB that we wish to look at all the rows in column 100. To look at rows 200 to 900 of column 100 of the *tfr* matrix, type the following at the prompt: `tfr(200:900,100)`. The `axis` command scales the plot to look at frequencies between 0 and 5000 Hz and amplitude values between 0 and 1.

```
>> help smt_plotSpec
>> smt_plotSpec(tfr(:,100),tfr_s,0,'lin')
>> axis([0 5000 0 1])
```

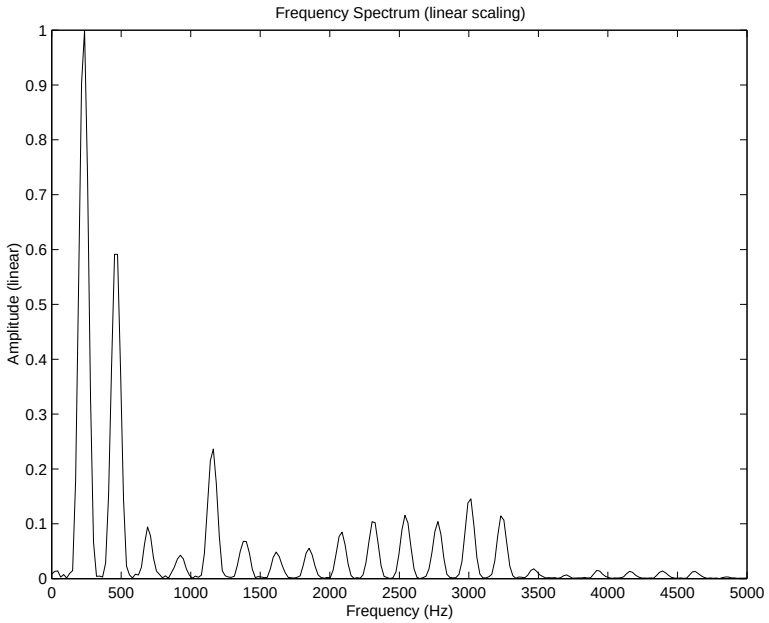

Figure 4.2: The frequency content in frame 100 of the STFT of the saxophone note.

4.4 Detect Peaks and Place Peaks

The `smt_detectPeaks` function takes a time-frequency representation and a time-frequency transform structure. Optional arguments can set the maximum number of peaks and the threshold. The function returns a peak matrix containing the peaks in each frame of the time-frequency representation.

The `smt_plotPeaks` function plots the calculated peaks on the time-frequency representation. Figure 4.3 shows the calculated peaks for the saxophone note from 50 to 850 ms and 0 to 5000 Hz; the peaks follow the harmonics closely. Notice that there are also peaks between the harmonics. These peaks come from noise and sidelobes of the window function and can be removed with the psychoacoustic model and track forming functions.

```
>> help smt_detectPeaks
>> tfrPeaks = smt_detectPeaks(tfr, tfr_s);
>> help smt_plotPeaks
>> smt_plotPeaks(tfrPeaks,tfr,tfr_s);
```

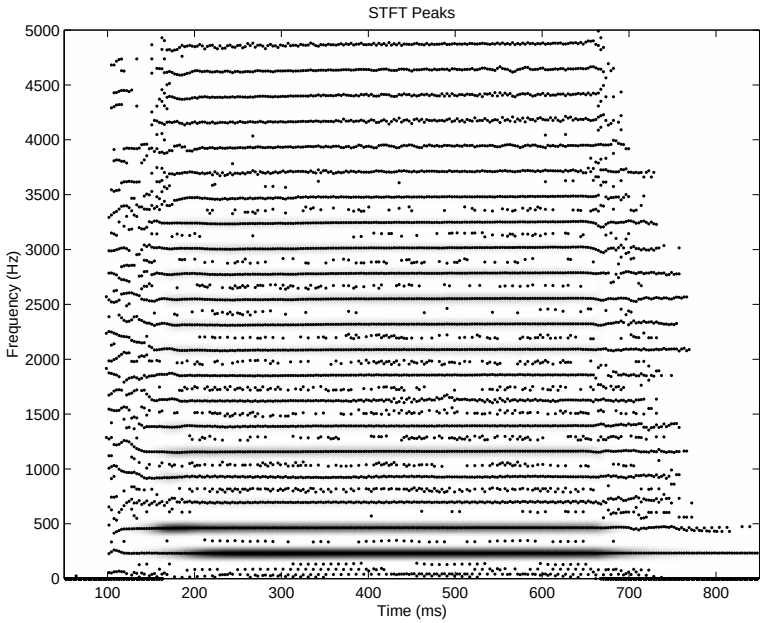

Figure 4.3: The smt_detectPeaks function returns the peaks in every frame of a time-frequency representation. Here the calculated peaks are plotted against the time-frequency representation.

```
>> axis([50 850 0 5000])
>> size(tfrPeaks)
ans =
    337 50  3
```

The peak matrix above is three dimensional; the first dimension specifies the frame, the second dimension specifies the peak, and the third dimension specifies amplitude, frequency, or phase. This peak matrix has 337 frames and up to 50 peaks.

The code below returns the amplitude, frequency, and phase values for the fourth peak in frame 100. The `squeeze` function removes unnecessary dimensions and the single quote displays the result as a row vector. The three numbers mean that the peak has an amplitude of -4.10 dB, a frequency of 462.93 Hz, and a phase of 2.51.

```
>> squeeze(tfrPeaks(100,4,:))'
```

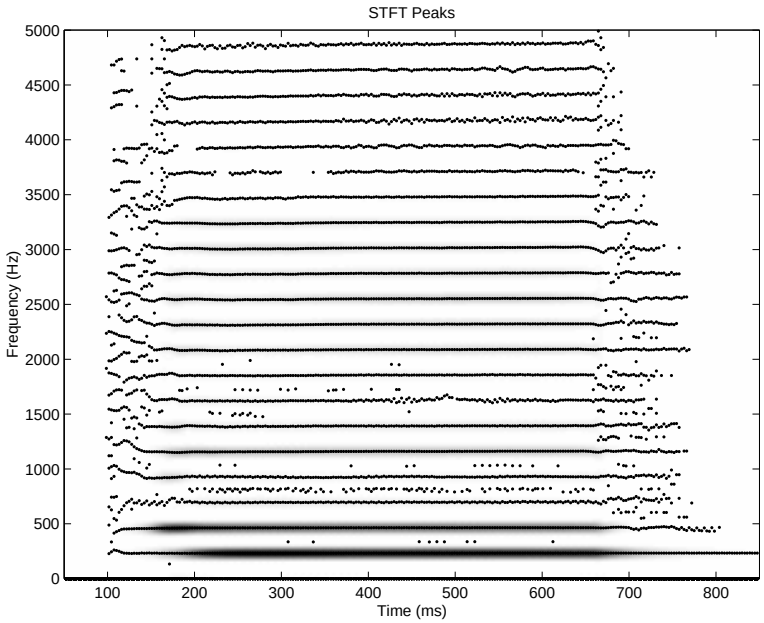

Figure 4.4: The psychoacoustic model uses the minimum audible field curve and masking to reduce the number of peaks in a peak matrix.

```
ans =
    -4.10   462.93  2.51
```

To synthesize a sound from a peak matrix, input the peak matrix into the `smt_placePeaks` function; the required inputs are the peak matrix and the time-frequency transform structure. It returns a time-frequency representation that can be synthesized with an inverse transform.

```
>> help smt_placePeaks
>> itfr = smt_placePeaks(tfrPeaks,tfr_s);
>> outSignal = smt_istft(itfr,tfr_s);
>> soundsc(outSignal,44100);
>> wavwrite(outSignal,44100,'outSignal.wav');
```

4.5 Psychoacoustic Model

The psychoacoustic model removes peaks from a peak matrix that the auditory system cannot detect. The first part of the function removes peaks that fall below the minimum audible field curve and the second part of the function

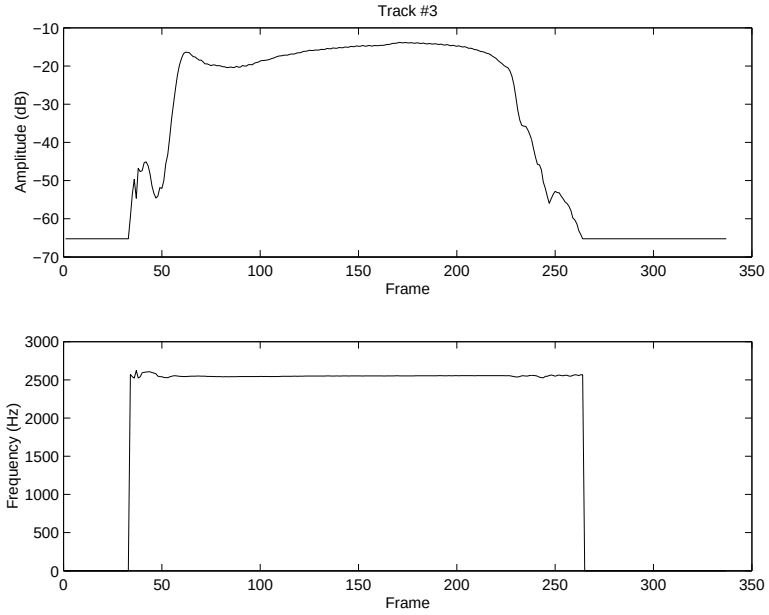

Figure 4.5: The smt_plotTrack command can plot the amplitude and frequency trajectory of a time-frequency track.

removes masked peaks. The `smt_psychModel` command takes a peak matrix as input and returns a peak matrix. An optional argument tells the function to use the masking routine.

4.6 TF Tracks

Figure 4.4 shows the result of running the psychoacoustic model. Compared to Figure 4.3, there are fewer peaks between harmonics. In the current psychoacoustic model, there are no masking curves for frequencies above 6030 Hz so high frequencies are attenuated.

```
>> help smt_psychModel
>> psychPeaks = smt_psychModel(tfrPeaks,1);
>> smt_plotPeaks(psychPeaks,tfr,tfr_s);
```

Up until this point, peaks have been grouped by frame. The `smt_tracks` function groups peaks by frequency, so the amplitude and frequency trajectory of a single partial can be tracked. The peaks are placed into tracks based on a

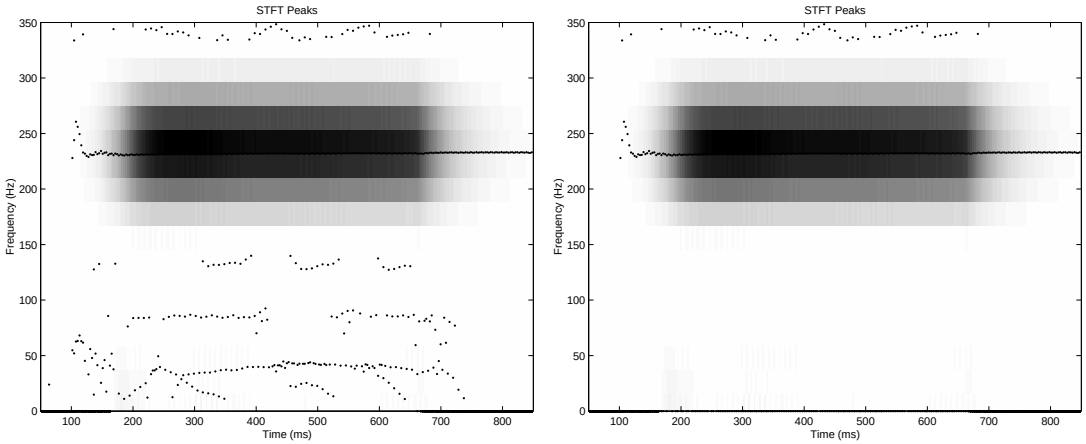

(a) Before Filtering

(b) After Filtering

Figure 4.6: The smt_filterPeaks function was used to filter the peaks between 0 and 150 Hz.

frequency threshold. After all peaks have been assigned to a track, the track list is pruned.

A track matrix is the same format as a peak matrix, so it can be plotted with the `smt_plotPeaks` command and resynthesized with the `smt_placePeaks` command.

To plot a particular track, use the `smt_plotTrack` command. It takes the track matrix and a number that specifies the track to plot. Track 3 of the *tfrTracks* matrix is shown in Figure 4.5.

```
>> help smt_tracks
>> tfrTracks = smt_tracks(tfrPeaks);
>> smt_plotTrack(tfrTracks,3);
>> itfr = smt_placePeaks(tfrTracks,tfr_s);
>> outSignal = smt_istft(itfr, tfr_s);
>> wavwrite(outSignal,44100,'outSignal.wav');
```

4.7 Modification Functions

Many modification functions can be found in the ModFunctions folder of the Toolbox; a complete list can be found by typing `help smt`. Each function has a different interface and I will only document one of the functions here. The `smt_filterPeaks` function takes a peak matrix, a frequency range, and an amplitude threshold. It removes peaks in the peak matrix that are within the frequency range and below the amplitude threshold.

The code below removes peaks between 0 and 150 Hz that are below 0 dB in amplitude. In other words, all peaks in that frequency range will be removed. Figure

```
>> help smt_filterPeaks
>> smt_plotPeaks(tfrPeaks,tfr,tfr_s)
>> axis([50 850 0 350])
>> filteredPeaks = smt_filterPeaks(tfrPeaks,[0 150],0);
>> smt_plotTFR(filteredPeaks,tfr,tfr_s)
>> axis([50 850 0 350])
```

4.8 Using Wavelets for Analysis and Synthesis

The Continuous Wavelet Transform using the Morlet wavelet can be computed with the `smt_cwt` command. This transform is similar to a Short-Time Fourier Transform with a Gaussian window that varies its width with frequency. The *N* parameter specifies the number of frequency samples and *wind* parameter sets the window width to a specific number of periods for each frequency. In the example below, I use 256 frequency samples and a window size of 16 periods.

The inverse transform is computed with `smt_icwt`. The CWT time-frequency representation can be put through the peak detection and track formation functions described above before resynthesis.

```
>> help smt_cwt
```

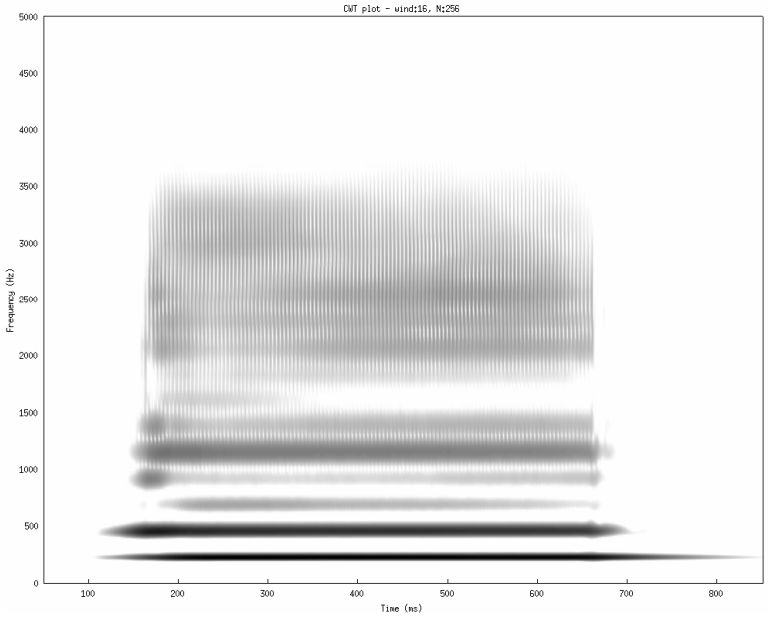

Figure 4.7: The CWT of the saxophone note.

```
>> [cwt, cwt_s] = smt_cwt(signal,256,16);
>> smt_plotTFR(cwt,cwt_s)
>> help smt_icwt
>> outSignal = smt_icwt(cwt,cwt_s);
```

5 Conclusions and Future Directions

The Spectral Modeling Toolbox is an environment for sound analysis, synthesis, and research. It is designed as a foundation for algorithm development and experimentation and the source code is available for anyone to download and use. I hope that other people will find it useful and contribute to the project by adding functions and improving algorithms.

The Toolbox is a learning system. I could have used existing systems to analyze and synthesize sounds, but I chose to implement the algorithms myself to gain a better understanding of the details. The code is heavily commented and some of the functions favor simpler, rather than more robust, solutions. While I would like them improved, I hope to keep some of the original algorithms in the Toolbox for pedagogic reasons; other people may benefit from the simple approach.

This thesis was also written favoring the simple approach. I have presented an overview of the Toolbox and a guide for using it without going too far into the details of the individual algorithms. Since the complete commented source code is available, I felt no need to describe the algorithms in the body of the thesis; the code itself and the comments are the best possible documentation. The Spectral Modeling Toolbox is a resource for learning about sound analysis and synthesis and I hope the approach of this thesis will provide a foundation for further study and experimentation.

As stated in the Introduction, one of the reasons I chose to study analysis/synthesis systems is because I believe they are the first step towards artificial recognition and separation of sound sources. The fundamental idea behind the analysis stage is to transform a sound into a representation where the perceptually salient features are more easily accessible. In the case of the systems

described in this thesis, the sounds were transformed into time-frequency representations and the time-varying frequency content in the signal over time could be examined. Peaks were identified as salient features (at a low level) and extracted from the representation.

I believe the next step is to identify groups of peaks and form higher level connections. Sinusoidal tracks are one way of doing this, but I believe there are more general ways based on psychoacoustic theories. For example, the Gestalt principles of grouping can be applied to auditory data. Bregman outlined many clues that the auditory system uses to group data and an intelligent system could use these to determine the best possible grouping for a set of peaks [2]. This requires further investigation and I believe the Spectral Modeling Toolbox provides a decent framework for this type of research.

Those interested in sound analysis and synthesis should download the Toolbox and try it out. I would appreciate any comments and suggestions. Based on feedback and possibly other contributions, the design and functions in the Toolbox may change; please read the README file for the latest information.

References

[1] S. Handel, *Listening: An Introduction to the Perception of Auditory Events*. Cambridge, MA: The MIT Press, first ed., 1989.

[2] A. S. Bregman, *Auditory Scene Analysis*. Cambridge, MA: The MIT Press, second ed., 1990.

[3] C.-T. Chen, *Digital Signal Processing*. New York: Oxford University Press, Inc., first ed., 2001.

[4] D. Gabor, "Theory of communication," *Journal of the IEEE*, vol. 93, pp. 429–457, 1946.

[5] F. J. Harris, "On the use of windows for harmonic analysis with the discrete fourier transform," *Proceedings of the IEEE*, vol. 66, no. 1, pp. 51–84, 1978.

[6] P. Masri, A. Bateman, and N. Canagarajah, "A review of time-frequency representations with application to sound/music analysis-resynthesis," *Organised Sound*, vol. 2, no. 3, pp. 193–205, 1997.

[7] M. Akay and C. Mello, "Time-frequency and time-scale (wavelets) analysis methods: Design and algorithms," *Smart Engineering System Design*, vol. 1, pp. 77–94, 1998.

[8] I. Daubechies, *Ten Lectures on Wavelets*. Philadelphia: Society for Industrial and Applied Mathematics, first ed., 1992.

[9] O. Rioul and M. Vetterli, "Wavelets and signal processing," *IEEE Signal Processing Magazine*, vol. 93, pp. 14–38, 1946.

[10] R. Kronland-Martinet, "The wavelet transform for analysis, synthesis, and

processing of speech and music sounds," *Computer Music Journal*, vol. 12, no. 4, pp. 11–20, 1988.

[11] B. Vercoe and et al., "Csound." `http://www.csound.org`, 2002.

[12] F. Auger, P. Flandrin, O. Lemoine, and P. Gonçalvès, "Time-frequency toolbox for matlab." `http://crttsn.univ-nantes.fr/~auger/tftb.html`, 1999.

[13] M. Dolson, "The phase vocoder: A tutorial," *Computer Music Journal*, vol. 10, no. 4, pp. 14–28, 1986.

[14] C. Penrose, "PVNation." `http://www.sfc.keio.ac.jp/~penrose/PVNation/index.html`, 2002.

[15] E. Lyon, "PowerPV." `http://arcana.dartmouth.edu/~eric/`, 2002.

[16] X. Serra and J. Smith III, "Spectral modeling synthesis: A sound analysis/synthesis system based on a deterministic plus stochastic decomposition," *Computer Music Journal*, vol. 14, no. 4, pp. 12–24, 1990.

[17] S. A. Gelfand, *Hearing*. New York: Marcel Dekker, Inc., third ed., 1998.

[18] B. Seeber, "Masking patterns from zwicker, jaroszewski and sonntag." `http://www.mmk.ei.tum.de/~see/msk/data.html`.

[19] E. Zwicker and A. Jaroszewski, "Inverse dependence of simultaneous tone-on-tone masking patterns at low levels," *Journal of the Acoustical Society of America*, vol. 71, no. 6, 1982.

A Basic Signal Processing in MATLAB

This appendix is an introduction to basic signal processing in MATLAB.

A.1 Sampling

Mathematically, a signal is often represented as a function of a time variable t. I will refer to such signals as *continuous-time* signals since the variable t is continuous (as opposed to discrete). For example, the continuous-time cosine wave with frequency ω_0 (in radians per second) is represented by $\cos(\omega_0 t)$. Often, it is convenient to represent the frequency in Hz instead of radians per second. This requires replacing ω_0 with $2\pi f_0$ as shown in (A.1).

$$\cos(\omega_0 t) = \cos(2\pi f_0 t) \tag{A.1}$$

To represent a signal in a computer, you must convert it into a discrete-time signal by a process called *sampling*. To sample a continuous-time signal, you replace the variable t with nT, where n is an integer and T is the sampling period in seconds. The sampled waveform, $x[n]$ is shown below.[1]

$$x[n] = \cos(2\pi f_0 nT) \tag{A.2}$$

In MATLAB, a sampled signal is computed in a form similar to its mathematical representation. In the code below, the `>>` is the MATLAB prompt. The code following the prompt can be typed directly into MATLAB or saved in a file and run as a script.

[1] A Note on Notation: Mathematicians often, but not always, distinguish between discrete-time functions and continuous-time functions with the choice of variable and choice brackets or parentheses. Continuous-time functions are often functions of a variable t (a real number), while discrete-time functions are often functions of a variable n (an integer). Additionally, continuous-time functions are written with parentheses $x(t)$, while discrete-time functions are written with brackets $x[n]$. Equation A.2 subtly shows the conversion of a continuous-time function into a discrete-time function: cos() is written with parentheses since it is a continuous-time function (though we are only considering the values at nT) and $x[n]$ is written with brackets since it is a discrete-time function.

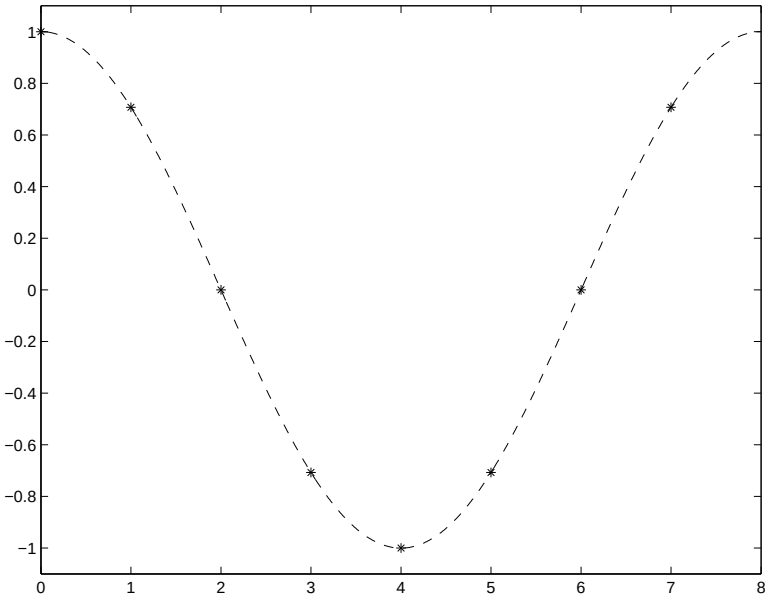

Figure A.1: A sampled cosine wave as stars. The dashed line shows a continuous cosine wave for reference.

```
>> n = 0:7;
>> T = 0.125;
>> f0 = 1;
>> x = cos( 2*pi*f0*n*T );
>> plot(n,x,'*')
```

The first line creates a vector of integers from 0 to 7 and stores them in the variable n. The second line sets our sampling period to 0.125 seconds; this is equivalent to a sampling rate of 8 samples per second. The third line sets our frequency variable to 1 Hz so the signal x should be one complete cycle of a cosine wave.[2] The plot function uses the values in n as the x-coordinates, uses the values in x as the y-coordinates, and plots the points as stars.

It is usually preferable to specify a sampling rate, F_s, instead of a sampling

[2]A Note on MATLAB: An important point to remember when using MATLAB is that every variable is a vector or a matrix. At the end of the code above, a vector was created and stored in the variable x. To access the elements of the vector, MATLAB uses parentheses. Be careful when accessing vectors because MATLAB numbers the locations starting with 1 instead of 0. Therefore, x(1) is the first sample of the cosine wave instead of x(0).

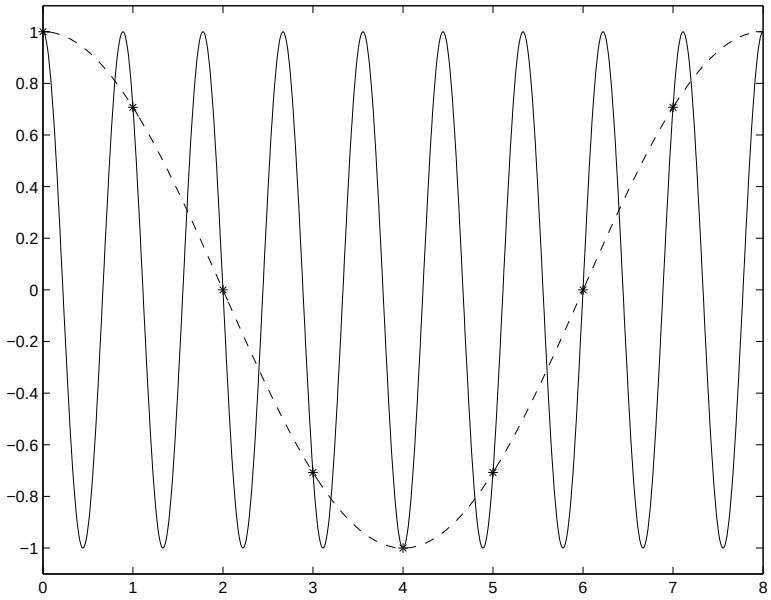

Figure A.2: Two continuous-time cosine waves that have the same discrete-time representation.

period. The sampling rate is the inverse of the sampling period, or $F_s = 1/T$. The code above can be easily changed to accomodate this.

```
>> n = 0:7;
>> Fs = 8;
>> f0 = 1;
>> x = cos( 2*pi*f0*n/Fs );
>> plot(n,x,'*')
```

Figure A.1 shows the difference between the discrete, or sampled, representation of the cosine wave and the continuous-time representation. Since only eight sample points are used to represent the continuous-time wave, it seems that other continuous-time waves could be represented by the same eight sample points. For example, Figure A.2 shows another continuous-time wave, at 9 Hz, that can be represented by the same eight sample points; a sampled signal does not uniquely specify a continuous-time signal.

The source of the problem is clear if we study Figure A.2: there are not

enough sample points to accurately represent the cosine with the greater frequency. In other words, the sampling rate is too slow and *aliasing*—high frequencies being represented by lower frequencies—occurs. This motivates the *Nyquist Sampling Theorem*, which states that the sampling rate must be greater than twice the highest frequency in the signal in order to accurately represent all the frequencies in the signal. The frequency that is twice the highest frequency in the signal is called the Nyquist frequency. By setting the sampling rate to 20 Hz, which is greater than the Nyquist frequency of 18 Hz, the two cosine waves will have the unique representations shown in Figure A.3. The code below creates these two cosine waves and plots them in the same figure.

```
>> n = 0:19;
>> Fs = 20;
>> f0 = 1;
>> x1 = cos( 2*pi*f0*n/Fs );
>> f1 = 9;
>> x2 = cos( 2*pi*f1*n/Fs );
>> subplot(2,1,1),plot(n,x1,'*')
>> subplot(2,1,2),plot(n,x2,'*')
```

Another way to look at sampling is to consider how the sampling rate affects the frequency content of the discrete-time signal. Figure A.2 showed that there is no one-to-one relationship between a sampled signal and a continuous time signal; a sampled signal could represent many different continuous-time signals. However, the Nyquist Sampling Theorem could also be stated in terms of frequency: frequencies above half the sampling rate cannot be accurately represented after sampling. In other words, the process of sampling limits the range of frequencies in a signal to $[-F_s/2, F_s/2)$, where F_s is the sampling rate. This range of frequencies is called the *Nyquist Interval*.

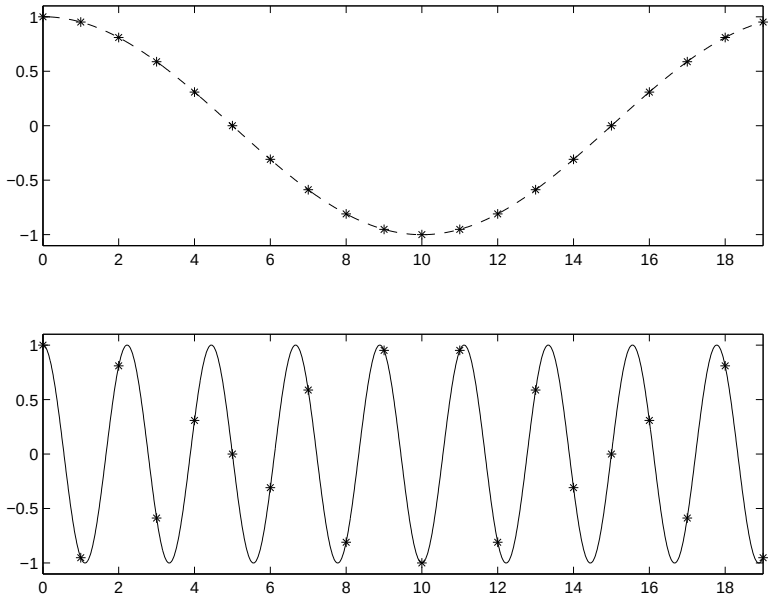

Figure A.3: The two continuous-time cosine waves have different discrete-time representations when sampled above the Nyquist frequency.

A.2 The Complex Exponential

Imagine a car moving around a circular track at a constant speed. Every time the car passes the starting point, it completes one lap. The distance the car travels per lap is equal to the circumference of the track ($2\pi r$); if the radius of the track is 1 mile, then the car travels 2π (≈ 6.28) miles per lap. The speed of the car determines how many laps the car can complete in an hour. At 62.8 miles per hour, the car will complete 10 laps in an hour.

If we replace the auto racing terms with their mathematical equivalents, a new way of representing periodic motion emerges. Suppose we replace the car on a track with a point on a circle, as shown in Figure A.4. The starting point is at cartesian coordinate $(1, 0)$, the point on the circle furthest to the right. The point moves around the circle at a constant *angular velocity*, and each time it passes the starting point, it completes one *cycle* of its motion. The distance the point has traveled is 2π radians since the radius of the circle has a length of 1.

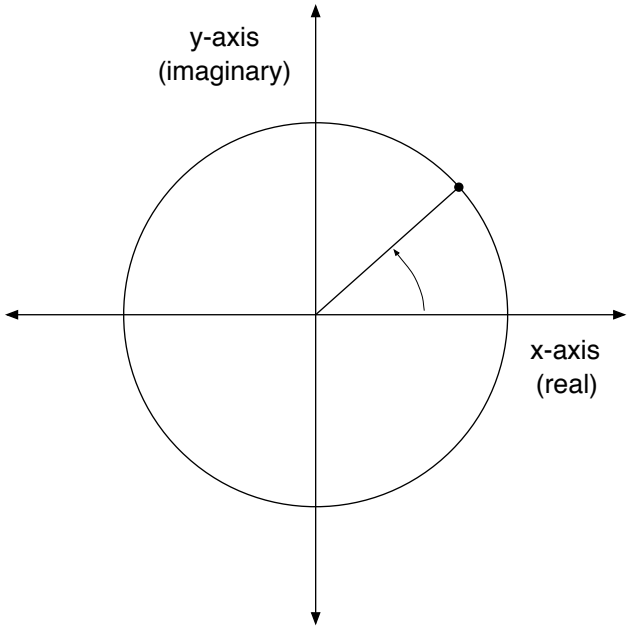

Figure A.4: Motion around a circle in the xy-plane can be represented by a complex exponential $e^{i\omega t}$ in the complex plane.

The angular velocity, in radians per second, determines how many cycles the point can complete in a second, or the *frequency* of the rotation. Therefore, a point moving around a circle can represent a frequency by the number of cycles it completes per second; a frequency of 200 Hz will be represented by a point moving fast enough to complete the 200 cycles in 1 second.

Mathematically, motion around a circle can be represented by a complex exponential function $e^{i\omega t}$, where ω is the angular velocity in radians per second. An equivalent representation is $e^{i2\pi ft}$, where f is the frequency in Hz. As t increases, the complex exponential will trace around the unit circle at a speed depending on the angular velocity ω or frequency f. The circle will lie in the complex plane, but that is essentially equivalent (isomorphic) to the xy or cartesian plane.

Euler related the cyclic motion of the complex exponential function to a

sine and a cosine with (A.3). This equation is called *The Euler Formula* and it can be expressed in either angular velocity ω or frequency f (its proof can be found in Appendix C). To visualize the relationship, first consider how the x coordinate of the point changes as the point moves around the circle; it traces out a cosine wave. If you focus on how the y coordinate changes, it is clear that it traces out a sine wave. So, the Euler Formula seems to be intuitively correct.

$$\begin{aligned} e^{i\omega t} &= \cos(\omega t) + i\sin(\omega t) \\ e^{2\pi i f t} &= \cos(2\pi f t) + i\sin(2\pi f t) \end{aligned} \tag{A.3}$$

Sampling a complex exponential in MATLAB is similar to sampling a cosine or any function. The code below samples a complex exponential with frequency 1 Hz and plots the real and imaginary parts separately; compare the real part to a cosine and the imaginary part to a sine.

```
>> n = 0:19;
>> Fs = 20;
>> f0 = 1;
>> x = exp( i*2*pi*f0*n/Fs );
>> subplot(2,1,1),plot(n,real(x),'*')
>> subplot(2,1,2),plot(n,imag(x),'*')
```

In this Appendix, frequencies will often be represented by complex exponentials, instead of sine or cosine waves, to simplify the Fourier analysis and interpretation. Simple formulas for representing sines and cosines in terms of complex exponentials are given in (A.4) and (A.5).

$$\sin\theta = \frac{e^{i\theta} - e^{-i\theta}}{2i} \tag{A.4}$$

$$\cos\theta = \frac{e^{i\theta} + e^{-i\theta}}{2} \tag{A.5}$$

A.3 Discrete Fourier Transform

The Fourier Transform shown (A.6) transforms a continuous-time function $x(t)$ into a continuous-frequency function $X(\omega)$. The same equation can also be written in terms of frequency f instead of angular velocity ω; this version is shown in (A.7). As mentioned above, a continuous-time function must be sampled in order to be represented in the computer. By the same reasoning, a continuous-frequency function must also be sampled in order to be represented in the computer.

$$X(\omega) = \int x(t)e^{-i\omega t}dt \tag{A.6}$$

$$X(f) = \int x(t)e^{-i2\pi ft}dt \tag{A.7}$$

In (A.7), the complex exponential is a function of time t and frequency f. To sample this function in time, replace t with nT, where T is the sampling period and n is an integer. The sampled complex exponential is then $e^{-i2\pi fnT}$.

To sample the frequency variable f, remember that sampling a signal in the time domain restricts the possible frequencies to a range of $[-F_s/2, F_s/2)$, where F_s is the sampling rate. The continuous range of frequencies from $-F_s/2$ to $F_s/2$ can be pictured as a line from $-F_s/2$ to $F_s/2$. This is shown in the top line of Figure A.5.

It is often more convenient to picture this range as positive frequencies from 0 to F_s. These two frequency ranges are equivalent when sampled at F_s because frequencies above $F_s/2$ will alias to negative frequencies. To sample the frequency range from $[0, F_s)$, let N be the number of frequency samples. Then the sequence $a_k = kF_s/N$, will be N evenly spaced frequency samples between 0 and F_s. A sampled frequency range for $N = 8$ and $F_s = 32$ is shown in Figure A.5.

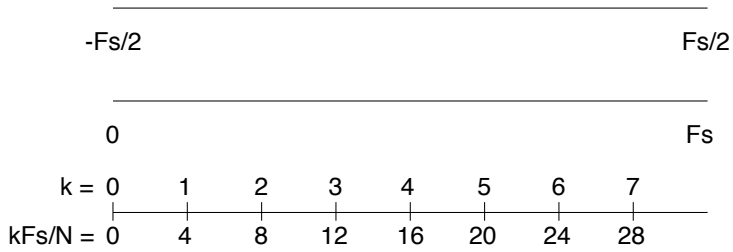

Figure A.5: The Nyquist Interval can be pictured as a line from $-F_s/2$ to $F_s/2$. That line is the same length as a line from 0 to F_s. To get N samples from 0 to F_s, let k be an integer from 0 to $N-1$ and choose the frequencies equal to kF_s/N. In the lowest line, $N = 8$ and $F_s = 32$.

Mathematically, sampling the time variable t and the frequency variable f of the Fourier Transform gives the Discrete Fourier Transform shown in (A.8). The conversion of the continuous transform into the discrete transform can be represented by the steps in A.9. The real derivation of the Discrete Fourier Transform from the Fourier Transform requires more rigor and is beyond the scope of this thesis.

$$X_d[k] = \sum_{n=0}^{N-1} x[n] e^{-i2\pi kn/N} \tag{A.8}$$

$$\begin{aligned} X(f) &= \int x(t) e^{-i2\pi ft} dt \\ &\rightarrow \sum_n x(nT) e^{-i2\pi fnT} \\ X(kF_s/N) &= \sum_n x(nT) e^{-i2\pi kF_s nT/N} \\ X[k] &= \sum_{n=0}^{N-1} x[n] e^{-i2\pi kn/N} \end{aligned} \tag{A.9}$$

The form of (A.8) is that of a scalar product. In Chapter 3, the inner product was introduced as the integral of the product of two functions. Essentially, the scalar, or dot, product is the discrete version of the inner product. It is calculated by summing the product of two discrete functions. In these terms,

the Discrete Fourier Transform can be seen as the dot product of the sampled signal $x[n]$ and the sampled basis functions $e^{-i2\pi kn/N}$. In $e^{-i2\pi kn/N}$, the $-2\pi k/N$ is the frequency and n is the sample index.

In MATLAB, it is easy to calculate the Discrete Fourier Transform of a sampled signal. If the length of the signal is a power of 2, MATLAB uses the *Fast Fourier Transform* (FFT), an efficient algorithm for calculating the DFT. The signals in the examples below will all be a power of 2 samples long.

```
>> N = 8;
>> Fs = 8;
>> n = 0:N-1;
>> f0 = 1;
>> x = exp( i*2*pi*f0*n/Fs );
>> X = fft(x);
>> round(X)
ans =
    0   8   0   0   0   0   0   0
```

In the code above, x is a sampled complex exponential with frequency 1 Hz. The FFT of x is zero everywhere except the second sample, which is equal to 8.

Suppose the frequency of the complex exponential is increased to 2 Hz. Then the FFT of x is zero everywhere except for the third sample. This is expected because we have sampled the frequency domain at kF_s/N. In these examples, $F_s/N = 1$, so a frequency of 2 Hz will be represented by a non-zero value at $X[2]$. Since MATLAB indexes the arrays starting with 1 instead of 0, the non-zero value occurs at $X(3)$.

```
>> N = 8;
>> Fs = 8;
>> n = 0:N-1;
>> f0 = 2;
```

```
>> x = exp( i*2*pi*f0*n/Fs );
>> X = fft(x);
>> round(X)
ans =
    0   0   8   0   0   0   0   0
>> round(X(3))
ans =
    8
```

Now suppose $N = 8$, and $F_s = 16$; then $F_s/N = 2$. This means the samples of the DFT will be spaced at intervals of 2 Hz. Suppose our complex exponential has frequencies at $f_0 = 2$ and $f_1 = 6$ Hz. Then we expect the DFT to be non-zero at $k = 1$ and $k = 3$. In MATLAB, $X(2)$ and $X(4)$ will be non-zero because arrrays start at index 1.

```
>> N = 8;
>> Fs = 16;
>> n = 0:N-1;
>> f0 = 2;
>> f1 = 6;
>> x = exp( i*2*pi*f0*n/Fs ) + exp( i*2*pi*f1*n/Fs );
>> X = fft(x);
>> round(X)
ans =
    0   8   0   8   0   0   0   0
```

The laws of the DFT tell us that the transform is linear. If x is multiplied by a scalar, then X will be multiplied by the same scalar. In the example below, multiplying x by 4 changes the value of $X(3)$ to 32.

```
>> N = 8;
>> Fs = 16;
>> n = 0:N-1;
```

```
>> f0 = 4;
>> x = 4*exp( i*2*pi*f0*n/Fs );
>> X = fft(x);
>> round(X)
ans =
    0   0   32  0   0   0   0   0
```

If we let $N = 16$ in the code above, then the frequency domain will be sampled at intervals of $F_s/N = 1$ Hz again and the non-zero sample will be found at $X(5)$ in MATLAB. The value at $X(5)$ has changed because of the change of N, the DFT size. This motivates normalization of the DFT by the DFT size (Appendix B will show that the normalization should use the window size when it is different from the DFT size).

```
>> N = 16;
>> Fs = 16;
>> n = 0:N-1;
>> f0 = 4;
>> x = 4*exp( i*2*pi*f0*n/Fs );
>> X = fft(x);
>> round(X)
ans =
    0   0   0   0   64  0   0   0   0   0   0   0   0   0   0   0
>> round(X)/N
ans =
    0   0   0   0   4   0   0   0   0   0   0   0   0   0   0   0
```

So far, we have seen that the frequency range of the DFT is sampled at intervals of F_s/N and that if the frequency of a complex exponential is an exact multiple of F_s/N, then the DFT will be zero everywhere except at one sample. The value of this sample will be the amplitude of the complex exponential multiplied by the DFT size. This is why it is common practice to normalize by the DFT size.

There are several basic concepts still left to cover. The first is that the values of the DFT are actually complex ($a \pm bi$). In the examples above, the b term was equal to zero and the round function was used to simplify the output. Typically, the b term is not zero and the complex values are converted into polar coordinates, or *magnitude* and *phase*. The MATLAB functions that convert a complex number to magnitude and phase are `abs` and `angle`.

```
>> N = 8;
>> Fs = 8;
>> n = 0:N-1;
>> f0 = 2;
>> x = 2*exp( i*2*pi*f0*n/Fs );
>> X = fft(x);
>> mag = abs(X)/N;
>> phs = angle(X);
>> mag
mag =
    0   0   2   0   0   0   0   0
>> phs
phs =
    2.36    2.75    -0.00   0.39    0.79    1.18    1.57    1.96
```

In the code above, all of the phase values except phs(3) should be ignored since the corresponding magnitude values are zero. Analyzing the phase will be discussed in Appendix B. Next, I will show what happens when the input signal is a sine wave or a cosine wave instead of a complex exponential.

```
>> N = 8;
>> Fs = 8;
>> n = 0:N-1;
>> f0 = 2;
>> sn = 2*sin( 2*pi*f0*n/Fs );
>> SN = fft(sn);
```

```
>> mag_sn = abs(SN)/N;
>> phs_sn = angle(SN);
>> mag_sn
mag_sn =
    0   0   1   0   0   0   1   0
>> phs_sn
phs_sn =
    0.00    0.78    -1.57   -0.79   0.00    0.79    1.57    -0.79
>> cs = 2*cos( 2*pi*f0*n/Fs );
>> CS = fft(cs);
>> mag_cs = abs(CS)/N;
>> phs_cs = angle(CS);
>> mag_cs
mag_cs =
    0   0   1   0   0   0   1   0
>> phs_cs
phs_cs =
    0.39    0.39    -0.00   0.00    0.00    -0.00   0.00    -0.39
```

When the signal is real, two samples of the DFT are non-zero: one for f_0 and the other for $-f_0$. Equations A.4 and A.5 show why this happens; a sine or cosine wave can be expressed as a sum of complex exponentials. These two signals are shown in Figure A.6. When analyzing real signals it is common to only view half of the frequency samples since the other half will have exactly the same information.

Suppose the frequency of the input signal is not an exact multiple of F_s/N. The DFT capable of representing any frequency between $[-F_s/2, F_s/2)$. The code below creates a sine wave with a frequency of 2.2 Hz. Comparing Figure A.7 to Figure A.6(a) shows that the peaks at SN(2) and SN(6) are still present but Figure A.7 also has energy at other samples. The spread of energy to frequency samples far from the peak is termed *spectral leakage*.

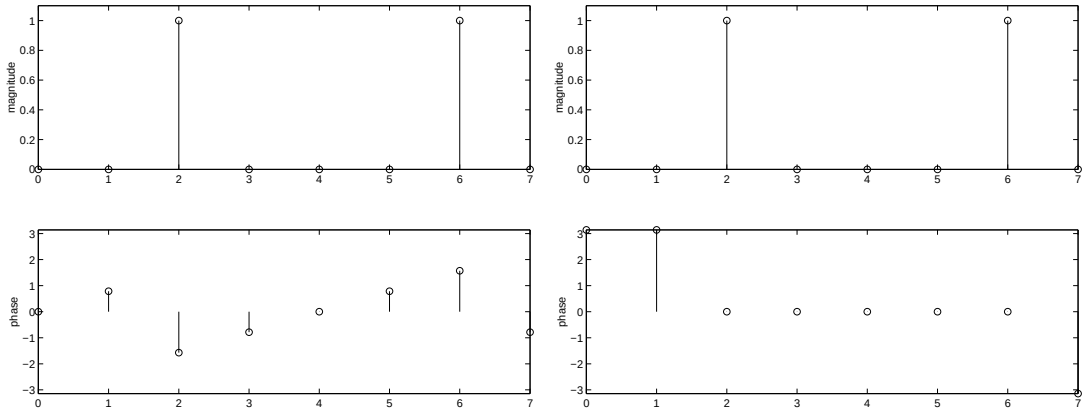

(a) The DFT of a sine wave

(b) The DFT of a cosine wave

Figure A.6: The DFT of a real sine or cosine wave is non-zero at positive and negative frequencies.

```
>> N = 8;
>> Fs = 8;
>> n = 0:N-1;
>> f0 = 2.2;
>> sn = 2*sin( 2*pi*f0*n/Fs );
>> SN = fft(sn);
>> mag_sn = abs(SN)/N;
>> phs_sn = angle(SN);
>> mag_sn
mag_sn =
    0.05    0.10    0.87    0.31    0.22    0.31    0.87    0.10
>> phs_sn
phs_sn =
    3.14   -1.77   -1.06    2.63    3.14   -2.63    1.06    1.77
```

In practice, the frequencies in the signals being analyzed are almost never perfect multiples of F_s/N so spectral leakage is a common occurrence. It can cause problems in analyzing the signal because the magnitude spectrum in Figure A.7 could have been produced by eight sine waves with different amplitudes. To

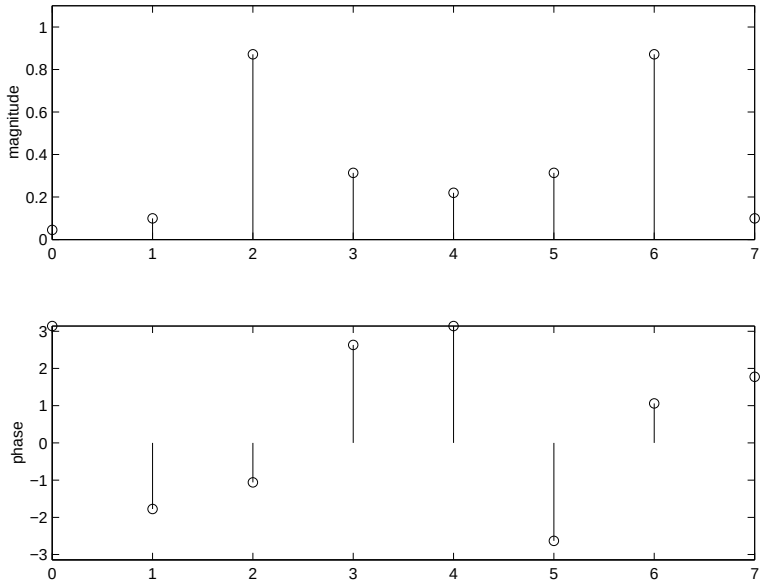

Figure A.7: The DFT of sine wave that is not an integer multiple of F_s/N will have energy at all frequencies. This is called *spectral leakage*.

minimize spectral leakage and improve the analysis, windows are often used.

A.4 Windows

Windowing minimizes the spread of energy from a single sine wave over the entire frequency domain.

Consider the sine wave created with the code below. Its magnitude spectrum is plotted in dB in Figure A.8(a). In this figure, we are only looking at the amplitudes of the positive frequencies between 190 and 250 Hz. Spectral leakage has occurred because the energy from this single sinusoid is significant at frequencies far from the actual frequency of the sinusoid.

```
>> N = 1024;
>> Fs = 1024;
>> n = 0:N-1;
>> f0 = 220.1;
>> sn = 2*sin( 2*pi*f0*n/Fs );
>> SN = fft(sn);
>> mag_sn = 20*log10(abs(SN)/N);
```

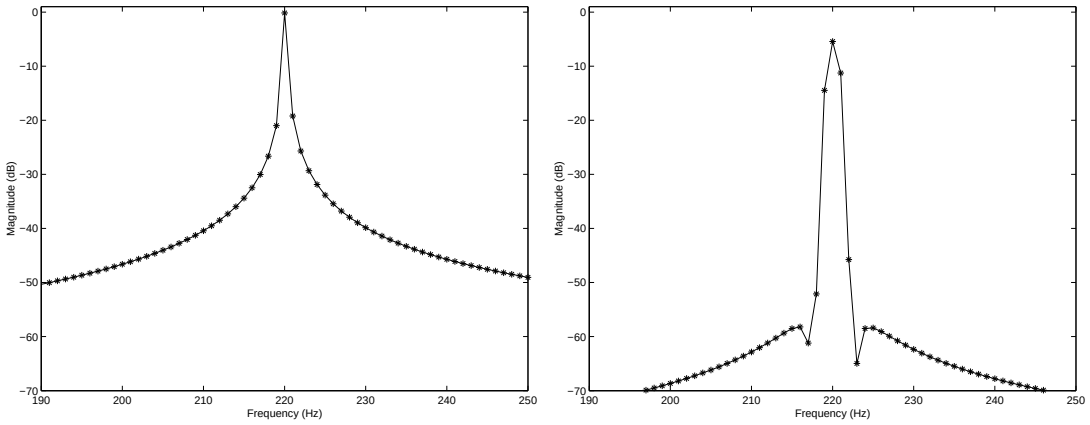

(a) A sine wave before windowing

(b) A sine wave after windowing

Figure A.8: The spectrum of a sine wave before and after windowing. The window has decreased the energy far from the peak but increased the width of the peak.

```
>> plot(n(1:512),mag_sn(1:512),'*-')
```

The code below creates the same sine wave at 220.1 Hz and multiplies it by a hamming window before taking the FFT. Figures 2.2 shows a hamming window and Figure 2.1 shows the result of multiplying a sine wave by a window. The spectrum of the windowed sinusoid is shown in Figure A.8(b).

```
>> N = 1024;
>> Fs = 1024;
>> n = 0:N-1;
>> f0 = 220.1;
>> h = hamming(N)';
>> sn = 2*sin( 2*pi*f0*n/Fs );
>> windowed = sn.*h;
>> WN = fft(windowed);
>> mag_wn = 20*log10(abs(WN)/N);
>> plot(n(1:512),mag_wn(1:512),'*-')
```

Figure A.8 illustrates the fundamental tradeoff of windowing. The energy

far from the peak has been decreased by the window, minimizing the effects of spectral leakage. The cost of windowing is an increased main lobe width, which can make close frequencies difficult to detect.

B Beyond the Basics

This appendix covers techniques for extracting accurate frequency, amplitude, and phase values from the DFT in MATLAB.

B.1 Parabolic Interpolation

Consider the sampled sinusoid created with the code below. It is 2048 points of a 220 Hz sine wave at a sampling rate of 44100 Hz. The `plot` command plots the magnitude spectrum, shown in Figure B.1. The `axis` command scales the plot to show frequency samples 7 to 16 and amplitude values 0 to 0.6.

```
>> Fs = 44100;
>> N = 2048;
>> n = 0:N-1;
>> f0 = 220;
>> h = hamming(N)';
>> sn = 2*sin( 2*pi*f0*n/Fs ).*h;
>> mag_sn = abs(fft(sn))/N;
>> plot(mag_sn(1:N/2),'*-')
>> axis([7 16 0 0.6])
```

The highest point in Figure B.1 occurs at frequency sample 11. Appendix A showed that the frequency domain of the DFT is sampled at intervals of F_s/N. In this case, every frequency bin is $F_s/N = 44100/2048 = 21.5332$ Hz apart, so the frequency in Hz at bin 11 is $10 * 21.5332 = 215.332$ Hz (remember that MATLAB numbers arrays starting at index 1). This value can also be found using the `max` command, which returns the maximum value in an array and its index.

```
>> [v,ix] = max(mag_sn);
v =
    0.5198
```

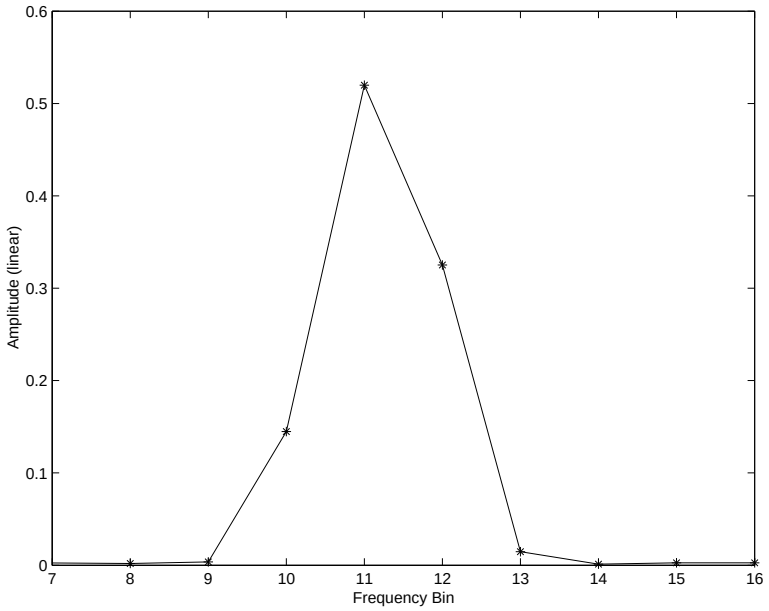

Figure B.1: The main peak in the magnitude spectrum of this sinusoid is at frequency sample 11.

```
ix =
    11
>> (ix-1)*Fs/N
ans =
    215.3320
>> f0-ans
ans =
    4.6680
```

The difference between the calculated frequency and the actual frequency was 4.668 Hz, which may or may not be significant depending on the required accuracy. One technique that always gives better results is parabolic interpolation.

Parabolic interpolation fits a parabola to the peak and the two adjacent samples. The vertex of the parabola is a better estimate of the frequency of the sinusoid than the location of the maximum sample.

Equation B.1 was derived from the equation for a parabola; the derivation can be found in Appendix C. In the equation, p is the offset of the vertex from the bin containing the peak, y_1 is the value of the point to the left of the peak, y_2 is the value of the peak, and y_3 is the value of the point to the right of the peak. The magnitude spectrum should be converted to decibels before using (B.1).

$$p = \frac{1}{2}\frac{y_1 - y_3}{y_1 - 2y_2 + y_3} \tag{B.1}$$

In MATLAB, we can find the value of p with the code below. To find the new frequency estimate, add p to $ix - 1$ and multiply by F_s/N.

```
>> y = 20*log10(mag_sn);
>> p = 1/2*(y(10) - y(12))/(y(10) - 2*y(11) + y(12))
p =
    0.2314
>> (p+ix-1)*Fs/N
ans =
    220.3159
```

Clearly, the frequency estimate is improved by parabolic interpolation. The amplitude of the vertex can also be calculated using (B.3). The MATLAB code below shows the original amplitude of the peak v in decibels and the new amplitude estimate b.

$$a = \frac{y_1 - y_2}{1 + 2p} \tag{B.2}$$

$$b = y_2 - ap^2 \tag{B.3}$$

```
>> [v,ix] = max(y)
v =
    -5.6834
ix =
    11
```

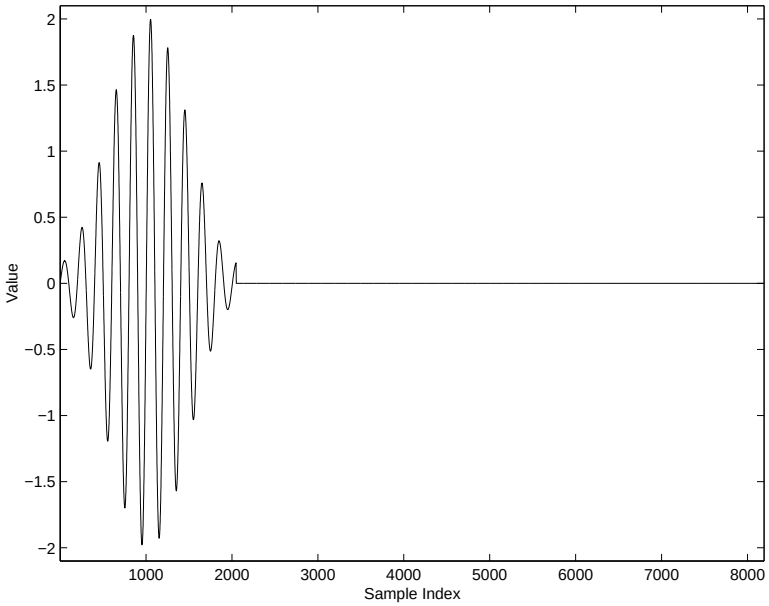

Figure B.2: The windowed sine wave is zero-padded to be 8192 samples long.

```
>> a = (y(ix-1) - y(ix))/(1+2*p);
>> b = y(ix) - 2*a*p^2
b =
    -4.8703
```

B.2 Zero-Padding

In all the examples so far, the window size has been the same as the FFT size. Zero-padding allows the window size and the FFT size to be different; zeros are added to the end of the windowed signal before taking the FFT. In the code below, N is the FFT size and M is the window size.

```
>> Fs = 44100;
>> N = 8192;
>> M = 2048
>> n = 0:M-1;
>> f0 = 220;
>> h = hamming(M)';
>> sn = 2*sin( 2*pi*f0*n/Fs ).*h;
>> sn(N) = 0;
```

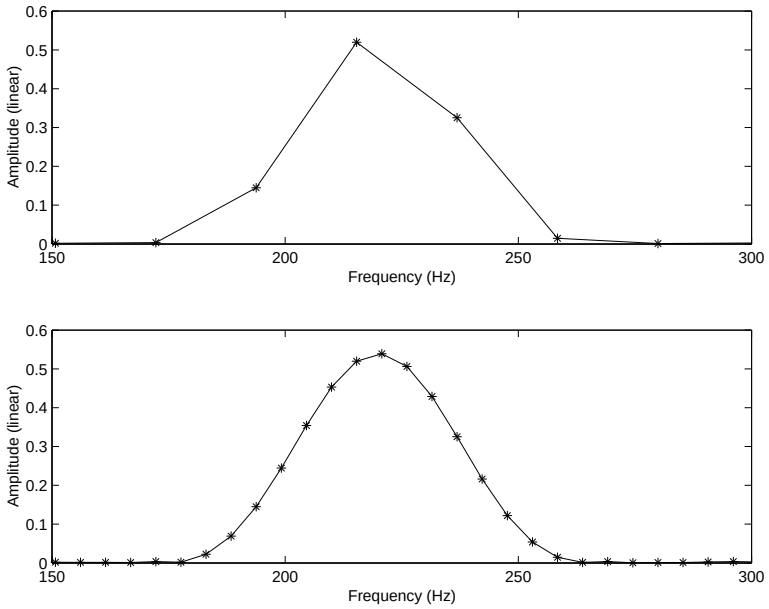

Figure B.3: The spectrum of the original signal compared to the spectrum of the zero-padded signal. Zero-padding causes interpolation in the frequency domain, resulting in a smoother peak.

```
>> plot(sn)
```

Figure B.3 compares the spectrum of the zero-padded signal to the original. Zero-padding does not change the frequency content of the original signal (zeros have no frequency content), but it does cause interpolation in the frequency domain. The result is a smoother peak.

The code below generated Figure B.3. In this code, zero-padding is achieved by telling the `fft` function to take a larger FFT than the length of the signal. The magnitude spectra are normalized by the window size and not the FFT size.

```
>> Fs = 44100;
>> N = 8192;
>> M = 2048
>> n = 0:M-1;
>> f0 = 220;
```

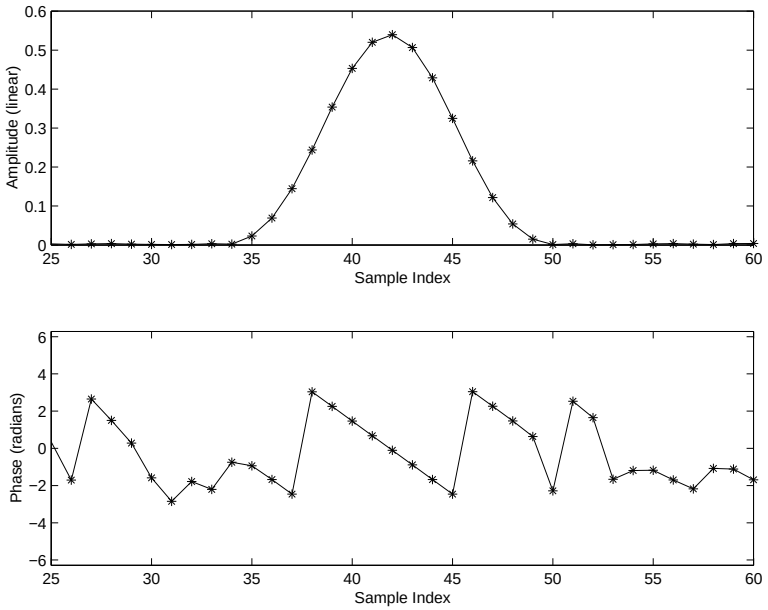

Figure B.4: The phase values under the peak lie on a line with constant slope.

```
>> h = hamming(M)';
>> sn = 2*sin( 2*pi*f0*n/Fs ).*h;
>> mag_sn = abs(fft(sn,M))/M;
>> mag_zero = abs(fft(sn,N))/M;
>> freq_sn = [0:M/2-1]'*Fs/M;
>> freq_zero = [0:N/2-1]'*Fs/N;
>> subplot(2,1,1),plot(freq_sn,mag_sn(1:M/2),'*-')
>> axis([150 300 0 0.6])
>> subplot(2,1,2),plot(freq_zero,mag_zero(1:N/2),'*-')
>> axis([150 300 0 0.6])
```

B.3 Centering the FFT Buffer for Phase Estimation

Consider the phase spectrum of cosine wave created by the code below and shown in Figure B.4. The phase values under the peak lie on a sloped line. This makes analysis difficult because it is not clear which of the values to use or if the slope of the line is important.

```
>> Fs = 44100;
```

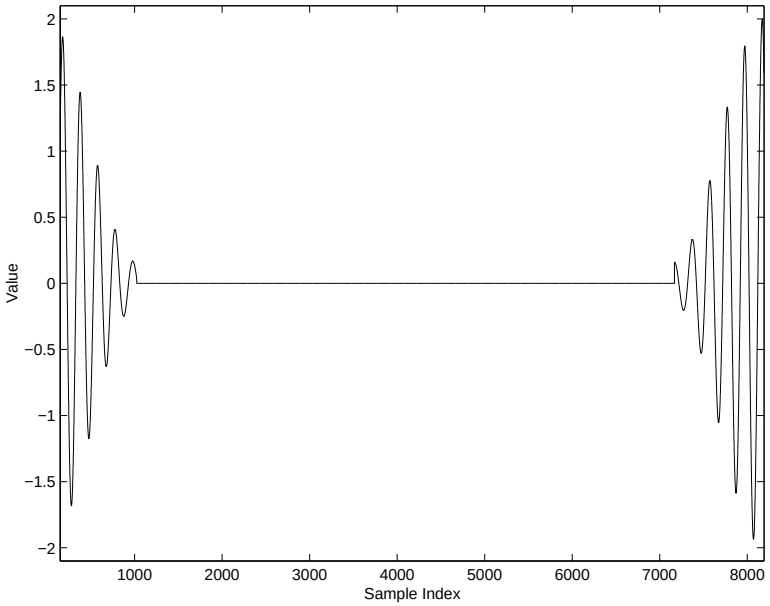

Figure B.5: The signal is shifted in the buffer so that the zeros are in the middle.

```
>> N = 8192;
>> M = 2048;
>> n = 0:M-1;
>> f0 = 220;
>> h = hamming(M)';
>> cs = 2*cos( 2*pi*f0*n/Fs ).*h;
>> mag_cs = abs(fft(cs,N))/M;
>> phs_cs = angle(fft(cs,N));
>> subplot(2,1,1),plot(mag_cs(1:N/2),'*-')
>> axis([25 60 0 0.6])
>> subplot(2,1,2),plot(phs_cs(1:N/2),'*-')
>> axis([25 60 -2*pi 2*pi])
```

To make analysis easier, the zero-padded signal can be shifted before taking the FFT. The effect of this is shown in Figure B.5; compare this to Figure B.2. Shifting the signal puts the first half of the signal at the end of the buffer and the last half of the signal at the beginning of the buffer. This means the extra zeros from zero-padding are in the middle. The code below can be used to

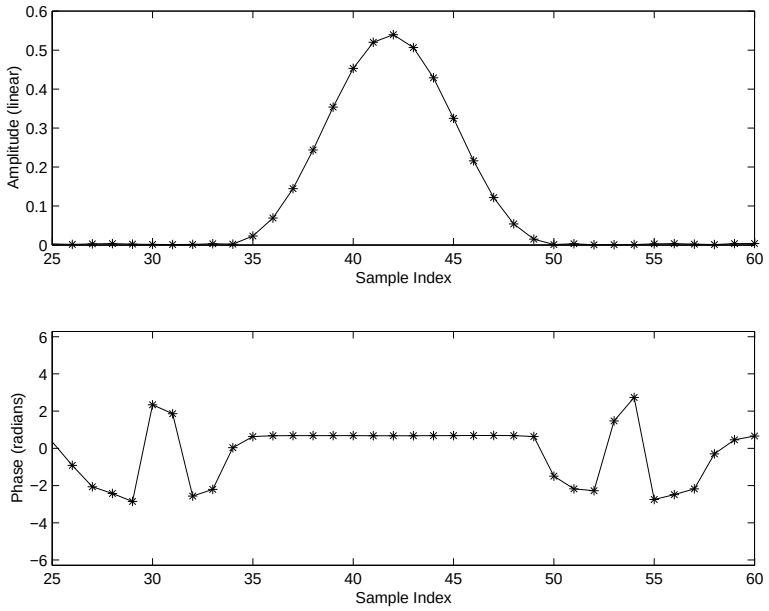

Figure B.6: The phase values under the peak lie on a horizontal line, facilitating phase estimation.

arrange the samples in this way.

```
>> center = ceil((M+1)/2);
>> buffer = zeros(N,1);
>> buffer(1:(M-center+1)) = cs(center:M);
>> buffer(N-center+2:N) = cs(1:center-1);
>> plot(buffer)
```

Figure B.6 shows the result of this shift on the phase spectrum. All the phase samples under the peak lie on a horizontal line so phase estimation is easier. The code below was used to create Figure B.6.

```
>> mag_shift = abs(fft(buffer,N))/M;
>> phs_shift = angle(fft(buffer));
>> subplot(2,1,1),plot(mag_shift(1:N/2),'*-')
>> axis([25 60 0 0.6])
>> subplot(2,1,2),plot(phs_shift(1:N/2),'*-')
>> axis([25 60 -2*pi 2*pi])
```

The final point to consider is how the phase values on the horizontal line in Figure B.6 relate to the phase offset of the sinusoid. Suppose we make a cosine wave with a phase offset of $\pi/4$ or 0.7854 using the code below. The magnitude and phase values near the peak are shown in Figure B.7.

```
>> Fs = 44100;
>> N = 8192;
>> M = 2048;
>> n = 0:M-1;
>> f0 = 220;
>> h = hamming(M)';
>> cs = 2*cos( 2*pi*f0*n/Fs + pi/4).*h;
>> buffer = zeros(N,1);
>> center = ceil((M+1)/2);
>> buffer(1:(M-center+1)) = cs(center:M);
>> buffer(N-center+2:N) = cs(1:center-1);
>> mag_cs = abs(fft(buffer))/M;
>> phs_cs = angle(fft(buffer));
>> phs_cs(40:45)'
ans =
1.4658 1.4657 1.4659 1.4664 1.4672 1.4682
```

The phase values under the peak are all approximately 1.47 radians and the phase offset of the cosine wave is 0.7854 radians. How do these values relate?

The shift property of the Fourier Transform states that the spectrum of a left shifted signal is $e^{i\omega\gamma}$ multiplied by the spectrum of the unshifted signal, where γ is the amount of shift in seconds; this relationship is derived in Appendix C. In other words, shifting the input signal by γ will add $\omega\gamma$ to the phase values of the spectrum.

To convert $\omega\gamma$ into a more useful form, first substitute $2\pi f$ for ω. This gives $2\pi f\gamma$. In the code above, we shifted the cosine by $M/2$ samples (half a window

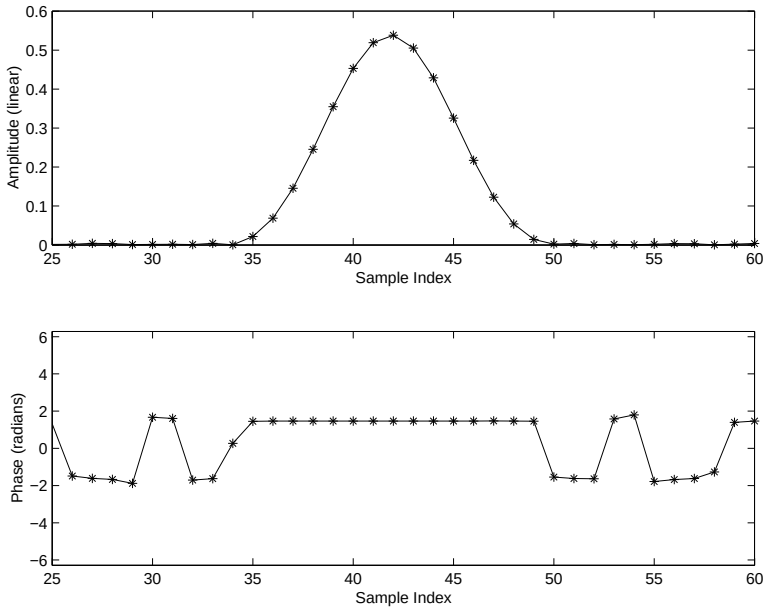

Figure B.7: The phase values form a nonzero horizontal line under the peak.

length). Therefore, γ is equal to $M/(2F_s)$ seconds. Appendix A established that the frequency domain of the DFT was sampled at intervals of F_s/N, so $f = kF_s/N$, where k is the sample, or bin, number. Substituting both of these relationships into $2\pi f\gamma$, we get $2\pi kF_sM/(2NF_s) = \pi kM/N$

First I will estimate the bin number (k) using parabolic interpolation. This value can be used in $\pi kM/N$ to determine the amount of phase that was added due to the shift. Subtracting this value from the phase under the peak gives an estimate of the phase offset of the cosine.

```
>> y = 20*log10(mag_cs);
>> [v,ix] = max(y);
>> p = 1/2*(y(ix-1) - y(ix+1))/(y(ix-1) - 2*y(ix) + y(ix+1));
>> k = ix-1+p;
>> phs = phs_cs(ix) - pi*k*M/N;
>> mod(phs, 2*pi)
ans =
    0.7879
```

```
>> pi/4
ans =
    0.7854
```

This Appendix has shown techniques for extracting accurate frequency, amplitude, and phase values from the Discrete Fourier Transform of a signal.

C Important Mathematical Proofs and Derivations

C.1 The Euler Formula

The Euler Formula shown in equation C.1 can be established through integration.

$$e^{i\theta} = \cos\theta + i\sin\theta \tag{C.1}$$

Let $z = \cos\theta + i\sin\theta$.

Then $dz/d\theta = -\sin\theta + i\cos\theta = i(i\sin\theta + \cos\theta)$.

So $dz/d\theta = iz$ or $dz/z = id\theta$.

Integrate both sides:

$$\begin{aligned}
\int dz/z &= \int id\theta \\
\ln z &= i\theta \\
e^{\ln z} &= e^{i\theta} \\
z &= e^{i\theta} \\
\cos\theta + i\sin\theta &= e^{i\theta}
\end{aligned}$$

C.2 Parabolic Interpolation

$$y(x) = a(x-p)^2 + b \tag{C.2}$$

$$\begin{aligned}
y_1 &= a(x_1-p)^2 + b \\
y_2 &= a(x_2-p)^2 + b \\
y_3 &= a(x_3-p)^2 + b
\end{aligned}$$

In our case, $x_1 = x_2 - 1$ and $x_3 = x_2 + 1$ so we can write the formulas above as

$$y_1 = a(-1-p)^2 + b$$

$$\begin{aligned} y_2 &= a(0-p)^2 + b \\ y_3 &= a(1-p)^2 + b \end{aligned}$$

Multiplying out, we get

$$\begin{aligned} y_1 &= a(1+2p+p^2) + b \\ y_2 &= ap^2 + b \\ y_3 &= a(1-2p+p^2) + b \end{aligned}$$

We can solve for p^2 in the second equation

$$p^2 = \frac{y_2 - b}{a} \tag{C.3}$$

Plug that into Equations 1 and 3

$$\begin{aligned} y_1 &= a\left(1+2p+\frac{y_2-b}{a}\right) + b \\ y_1 &= a + 2pa + y_2 \\ y_3 &= a\left(1-2p+\frac{y_2-b}{a}\right) + b \\ y_3 &= a - 2pa + y_2 \end{aligned}$$

Solve for a in both equations

$$\begin{aligned} a &= \frac{y_1 - y_2}{1+2p} \\ a &= \frac{y_3 - y_2}{1-2p} \end{aligned}$$

Set these equations equal to each other

$$\begin{aligned} \frac{y_1 - y_2}{1+2p} &= \frac{y_3 - y_2}{1-2p} \\ (y_1 - y_2)(1-2p) &= (y_3 - y_2)(1+2p) \\ y_1 - y_2 - 2py_1 + 2py_2 &= y_3 - y_2 + 2py_3 - 2py_2 \end{aligned}$$

$$
\begin{aligned}
y_1 - 2py_1 + 2py_2 &= y_3 + 2py_3 - 2py_2 \\
-2py_3 + 2py_2 - 2py_1 + 2py_2 &= y_3 - y_1 \\
2p(2y_2 - y_3 - y_1) &= y_3 - y_1 \\
2p &= \frac{y_3 - y_1}{2y_2 - y_3 - y_1} \\
p &= \frac{1}{2}\frac{y_1 - y_3}{y_1 - 2y_2 + y_3}
\end{aligned}
$$

Then

$$a = \frac{y_1 - y_2}{1 + 2p} \tag{C.4}$$

and

$$b = y_2 - ap^2 \tag{C.5}$$

C.3 Shift Property of the Fourier Transform

$$X(\omega) = \int x(t)e^{-i\omega t}dt \tag{C.6}$$

$x(t+\gamma)$ is $x(t)$ shifted to the left by γ. Let $\tau = t+\gamma$, then $d\tau = dt$ and $t = \tau - \gamma$.

$$
\begin{aligned}
\int x(t+\gamma)e^{-i\omega t}dt &= \int x(\tau)e^{-i\omega(\tau-\gamma)}d\tau \\
&= \int x(\tau)e^{-i\omega\tau}e^{i\omega\gamma}d\tau \\
&= e^{i\omega\gamma}\int x(\tau)e^{-i\omega\tau}d\tau \\
&= e^{i\omega\gamma}X(\omega)
\end{aligned}
$$

Therefore, shifting the signal $x(t)$ in time by γ multiplies its Fourier Transform by $e^{i\omega\gamma}$. This will affect the phase of the Transform but not the magnitude.

Bibliography

Akay, M. and Mello, C., "Time-Frequency and Time-Scale (Wavelets) Analysis Methods: Design and Algorithms," *Smart Engineering System Design*, vol. 1, pp. 77–94, 1998.

Auger, F., Flandrin, P., Lemoine, O., and Gonçalvès, P., "Time-Frequency Toolbox for MATLAB," `http://crttsn.univ-nantes.fr/~auger/tftb.html`, 1999.

Bregman, A. S., *Auditory Scene Analysis*. Cambridge, MA: The MIT Press, second ed., 1990.

Chen, C.-T., *Digital Signal Processing*. New York: Oxford University Press, Inc., first ed., 2001.

Daubechies, I., *Ten Lectures on Wavelets*. Philadelphia: Society for Industrial and Applied Mathematics, first ed., 1992.

Dolson, M., "The Phase Vocoder: A Tutorial," *Computer Music Journal*, vol. 10, pp. 14–28, 1986.

Gabor, D., "Theory of Communication," *Journal of the IEEE*, vol. 93, pp. 429–457, 1946.

Gelfand, S. A., *Hearing*. New York: Marcel Dekker, Inc., third ed., 1998.

Handel, S., *Listening: An Introduction to the Perception of Auditory Events*. Cambridge, MA: The MIT Press, first ed., 1989.

Harris, F. J., "On the Use of Windows for Harmonic Analysis with the Discrete Fourier Transform," *Proceedings of the IEEE*, vol. 66, pp. 51–84, 1978.

Kronland-Martinet, R., "The Wavelet Transform for Analysis, Synthesis, and Processing of Speech and Music Sounds," *Computer Music Journal*, vol. 12, pp. 11–20, 1988.

Lyon, E., "PowerPV," http://arcana.dartmouth.edu/~eric/, 2002.

Masri, P., Bateman, A., and Canagarajah, N., "A review of time-frequency representations with application to sound/music analysis-resynthesis," *Organised Sound*, vol. 2, pp. 193–205, 1997.

Penrose, C., "PVNation," http://www.sfc.keio.ac.jp/~penrose/PVNation/index.html, 2002.

Rioul, O. and Vetterli, M., "Wavelets and Signal Processing," *IEEE Signal Processing Magazine*, vol. 93, pp. 14–38, 1946.

Seeber, B., "Masking patterns from Zwicker, Jaroszewski and Sonntag," http://www.mmk.ei.tum.de/~see/msk/data.html.

Serra, X. and Smith III, J., "Spectral Modeling Synthesis: A Sound Analysis/Synthesis System Based on a Deterministic plus Stochastic Decomposition," *Computer Music Journal*, vol. 14, pp. 12–24, 1990.

Vercoe, B. and et al., "Csound," http://www.csound.org, 2002.

Zwicker, E. and Jaroszewski, A., "Inverse dependence of simultaneous tone-on-tone masking patterns at low levels," *Journal of the Acoustical Society of America*, vol. 71, 1982.